Whitepaper:

The Linear Boltzmann Solver - a Discrete Ordinates Method solver - Theory Manual

August, 2022

Jan Vermaak

Rev 1.12

χtech
Simulation Engine

Contents

List of Figures

1 Basics - The Linear Boltzmann Transport Equation

Let us denote the position of a particle in space by $\mathbf{x} = [x \; y \; z]$ and the direction along which it is traveling by the normal vector $\mathbf{\Omega}$ such that

$$\mathbf{\Omega} = [\Omega_x, \Omega_y, \Omega_z] = [\sin\theta\cos\varphi, \quad \sin\theta\sin\varphi, \quad \cos\theta],$$
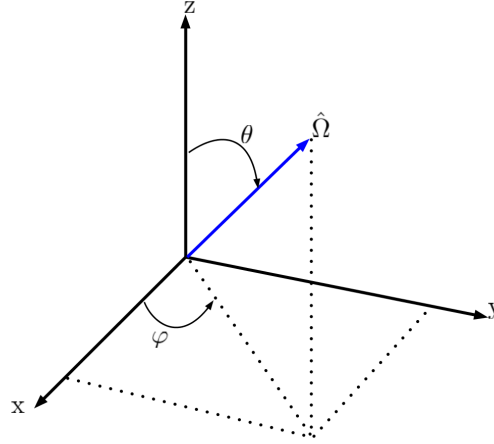
Figure 1.1: Orientation of direction in cartesian space.

where φ denotes the **azimuthal-angle** and θ denotes the **polar-angle**. In many instances it is beneficial to use the azimuthal- and polar-angles rather than the direction vector but that only happens later in this text. Now, we want to observe a control volume V, with surface S, and the balance of particles within it. But first we have to define a few terms. First is the particle density n, with units $[\frac{particles}{cm^3}]$. The particles we are referring to here can certainly exist at any energy- or velocity, any direction of travel and could also represent an average over some time interval. In order to comprehend the basic nature of these particles we have to classify these particles according the properties they are endowed with. To this end we extend the particle density to depend on position, $\mathbf{x}$, energy, E, direction, $\mathbf{\Omega}$, and time, t, written as

$$n(\mathbf{x}, E, \mathbf{\Omega}, t),$$

which now has units of $\left[\frac{particles}{cm^3 - eV - steridian}\right]$. Particle density can be multiplied by the velocity, v, associated with its energy to define the angular flux ψ, written as

$$\psi(\mathbf{x}, E, \mathbf{\Omega}, t) = v(E) \; n(\mathbf{x}, E, \mathbf{\Omega}, t),$$

which now has units of $\left[\frac{particles}{cm^2 - eV - steridian - s}\right]$. The definition of the flux is essential to couple reactions to known cross sections in the form of a reaction rate, RR, defined as

$$RR(\mathbf{x}, E, \mathbf{\Omega}, t) = \sigma(\mathbf{x}, E, \mathbf{\Omega}, t)\psi(\mathbf{x}, E, \mathbf{\Omega}, t) \tag{1.1}$$

with units $\left[\frac{1}{cm^3-s-eV-steridian-s}\right]$, where σ is known as a **macroscopic cross section** with units $\left[\frac{1}{cm}\right]$.

Please note that, traditionally, the symbol for the macroscopic cross section is capital "sigma", Σ, which then incorporates the traditional symbol for the microscopic cross section, σ (units cm^2), as a product with the atom-density, N, with units $\frac{1}{cm^3}$, i.e., $\Sigma = N\sigma$. For simplicity we opted to use σ, instead of Σ, to represent the macroscopic cross section throughout this whitepaper.

Let us now turn our attention to the balance of particles in a control volume.
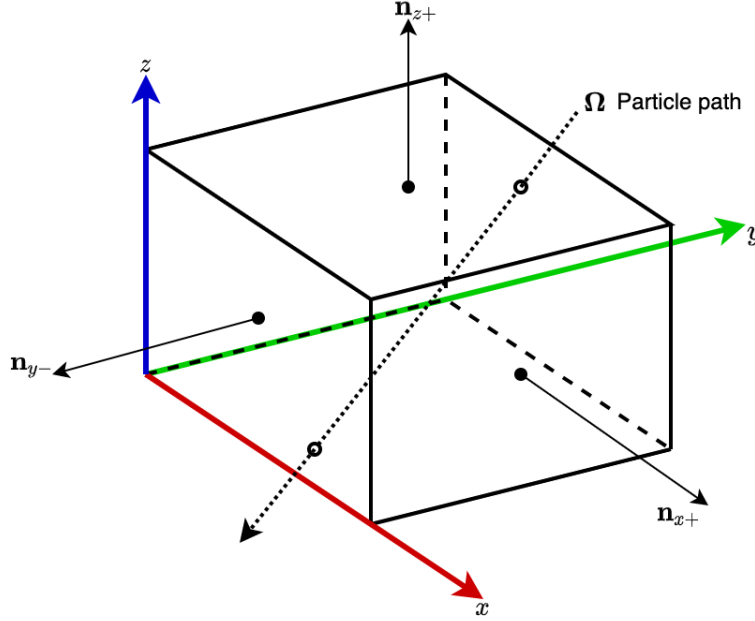
Figure 1.2: Control volume for neutron balance.

Consider the control volume as shown in figure 1.2 with outward pointing surface normal $\mathbf{n}$. The time rate of change of particles over the volume is given by the following terms:

Term A: Particles streaming inward or outward at the surface,

$$-\int_S \left[\mathbf{n\cdot\,\Omega}\psi(\mathbf{x}, E, \mathbf{\Omega}, t)\right]dA.$$

Note the sign on this term is negative because if the particles are streaming inward the dot-product of the angle and the normal will be negative.

Term B: Particles absorbed in the volume via an absorption reaction cross section, σ_a,

$$-\int_V \sigma_a(\mathbf{x}, E, t)\psi(\mathbf{x}, E, \mathbf{\Omega}, t)d\mathbf{x}$$

Term C: Particles scattering, with cross section σ_s, from the current energy E and angle $\mathbf{\Omega}$ to another energy E' and angle $\mathbf{\Omega}'$,

$$-\int_V \int_{E'} \int_{4\pi} \sigma_s(\mathbf{x}, E{\to}E', \mathbf{\Omega}{\to}\mathbf{\Omega}', t)\psi(\mathbf{x}, E, \mathbf{\Omega}, t)d\mathbf{\Omega}'dE'd\mathbf{x}$$

Term D: Particles scattering, with cross section σ_s, from all other energies E' and angles $\mathbf{\Omega}'$ to the current energy E and angle $\mathbf{\Omega}$,

$$+\int_V \int_{E'} \int_{4\pi} \sigma_s(\mathbf{x}, E' \to E, \mathbf{\Omega}' \to \mathbf{\Omega}, t)\psi(\mathbf{x}, E', \mathbf{\Omega}', t)d\mathbf{\Omega}' dE' d\mathbf{x}$$

Term E: Particles created from interactions with materials via the cross section σ_f. The number of particles created from an interaction at energy E' is denoted with $\bar{\nu}(E')$ and the continuous spectrum of resulting energy is χ with an isotropic angular distribution (hence $\frac{1}{4\pi}$). The formulation is then

$$+\frac{\chi(E)}{4\pi}\int_V \int_{E'} \int_{4\pi} \bar{\nu}(E')\sigma_f(\mathbf{x}, E', \mathbf{\Omega}', t)\psi(\mathbf{x}, E', \mathbf{\Omega}', t)d\mathbf{\Omega}' dE' d\mathbf{x}$$

Term F: Particles created from a volumetric source q.

$$+\int_V q(\mathbf{x}, E, \mathbf{\Omega})\ d\mathbf{x}, t.$$

Putting all these items together, we get

$$\int_V \frac{1}{v(E)}\frac{d}{dt}\Big(\psi(\mathbf{x}, E, \mathbf{\Omega}, t)\Big)d\mathbf{x} = -\int_S \Big[\mathbf{n}\cdot\mathbf{\Omega}\ \psi(\mathbf{x}, E, \mathbf{\Omega}, t)\Big]dA - \int_V \sigma_a(\mathbf{x}, E, t)\psi(\mathbf{x}, E, \mathbf{\Omega}, t)d\mathbf{x}$$

$$-\int_V \int_{E'} \int_{4\pi} \sigma_s(\mathbf{x}, E \to E', \mathbf{\Omega} \to \mathbf{\Omega}', t)\psi(\mathbf{x}, E, \mathbf{\Omega}, t)d\mathbf{\Omega}' dE' d\mathbf{x}$$

$$+\int_V \int_{E'} \int_{4\pi} \sigma_s(\mathbf{x}, E' \to E, \mathbf{\Omega}' \to \mathbf{\Omega}, t)\psi(\mathbf{x}, E', \mathbf{\Omega}', t)d\mathbf{\Omega}' dE' d\mathbf{x} \qquad (1.2)$$

$$+\frac{\chi(E)}{4\pi}\int_V \int_{E'} \int_{4\pi} \bar{\nu}(E')\sigma_f(\mathbf{x}, E', \mathbf{\Omega}', t)\psi(\mathbf{x}, E', \mathbf{\Omega}', t)d\mathbf{\Omega}' dE' d\mathbf{x}$$

$$+\int_V q(\mathbf{x}, E, \mathbf{\Omega}, t)d\mathbf{x}$$

after which we can apply Gauss's divergence theorem on the surface integral term,

$$\int_S \Big[\mathbf{n}\cdot\mathbf{\Omega}\ \psi(\mathbf{x}, E, \mathbf{\Omega}, t)\Big]dA = \int_V \Big[\mathbf{\nabla}\cdot\mathbf{\Omega}\psi(\mathbf{x}, E, \mathbf{\Omega}, t)\Big]d\mathbf{x}.$$

Now we have

$$\int_V \frac{1}{v(E)}\frac{d}{dt}\Big(\psi(\mathbf{x}, E, \mathbf{\Omega}, t)\Big)d\mathbf{x} = -\int_V \Big[\mathbf{\nabla}\cdot\mathbf{\Omega}\ \psi(\mathbf{x}, E, \mathbf{\Omega}, t)\Big]d\mathbf{x} - \int_V \sigma_a(\mathbf{x}, E, t)\psi(\mathbf{x}, E, \mathbf{\Omega}, t)d\mathbf{x}$$

$$-\int_V \int_{E'} \int_{4\pi} \sigma_s(\mathbf{x}, E \to E', \mathbf{\Omega} \to \mathbf{\Omega}', t)\psi(\mathbf{x}, E, \mathbf{\Omega}, t)d\mathbf{\Omega}' dE' d\mathbf{x}$$

$$+\int_V \int_{E'} \int_{4\pi} \sigma_s(\mathbf{x}, E' \to E, \mathbf{\Omega}' \to \mathbf{\Omega}, t)\psi(\mathbf{x}, E', \mathbf{\Omega}', t)d\mathbf{\Omega}' dE' d\mathbf{x} \qquad (1.3)$$

$$+\frac{\chi(E)}{4\pi}\int_V \int_{E'} \int_{4\pi} \bar{\nu}(E')\sigma_f(\mathbf{x}, E', \mathbf{\Omega}', t)\psi(\mathbf{x}, E', \mathbf{\Omega}', t)d\mathbf{\Omega}' dE' d\mathbf{x}$$

$$+\int_V q(\mathbf{x}, E, \mathbf{\Omega}, t)d\mathbf{x}.$$

Dropping all the $\int_V d\mathbf{x}$ and noting that $\boldsymbol{\nabla}\cdot\boldsymbol{\Omega}\ \psi(\mathbf{x},E,\boldsymbol{\Omega},t) = \boldsymbol{\Omega}\cdot\nabla\psi(\mathbf{x},E,\boldsymbol{\Omega},t)$ gives

$$
\begin{aligned}
\frac{1}{v(E)}\frac{d}{dt}\Big(\psi(\mathbf{x},E,\boldsymbol{\Omega},t)\Big) =& -\boldsymbol{\Omega}\cdot\nabla\psi(\mathbf{x},E,\boldsymbol{\Omega},t) - \sigma_a(\mathbf{x},E,t)\psi(\mathbf{x},E,\boldsymbol{\Omega},t) \\
& -\int_{E'}\int_{4\pi}\sigma_s(\mathbf{x},E{\to}E',\boldsymbol{\Omega}{\to}\boldsymbol{\Omega}',t)\psi(\mathbf{x},E,\boldsymbol{\Omega},t)d\boldsymbol{\Omega}'dE' \\
& +\int_{E'}\int_{4\pi}\sigma_s(\mathbf{x},E'{\to}E,\boldsymbol{\Omega}'{\to}\boldsymbol{\Omega},t)\psi(\mathbf{x},E',\boldsymbol{\Omega}',t)d\boldsymbol{\Omega}'dE' \\
& +\frac{\chi(E)}{4\pi}\int_{E'}\int_{4\pi}\bar{\nu}(E')\sigma_f(\mathbf{x},E',\boldsymbol{\Omega}',t)\psi(\mathbf{x},E',\boldsymbol{\Omega}',t)d\boldsymbol{\Omega}'dE' \\
& +q(\mathbf{x},E,\boldsymbol{\Omega},t).
\end{aligned}
\tag{1.4}
$$

If we leave the equation in this form we will need to perform the scattering integral over all energy groups where neutrons are scattering to this group, and another integral over all energy groups where neutrons are scattering from this group to another. To reduce the complexity/difficulty of this we combine the scattering from group E to E', and from angle $\boldsymbol{\Omega}$ to $\boldsymbol{\Omega}'$, into the total cross-section as

$$
\begin{aligned}
\sigma_t(\mathbf{x},E,\boldsymbol{\Omega},t)\psi(\mathbf{x},E,\boldsymbol{\Omega},t) =& \ \sigma_a(\mathbf{x},E,t)\psi(\mathbf{x},E,\boldsymbol{\Omega},t) \\
& +\int_{E'}\int_{4\pi}\sigma_s(\mathbf{x},E{\to}E',\boldsymbol{\Omega}{\to}\boldsymbol{\Omega}',t)\psi(\mathbf{x},E,\boldsymbol{\Omega},t)d\boldsymbol{\Omega}'dE',
\end{aligned}
$$

which gives us the basic time-dependent Linear Boltzmann Equation (LBE),

$$
\begin{aligned}
\frac{1}{v(E)}\frac{d}{dt}\Big(\psi(\mathbf{x},E,\boldsymbol{\Omega},t)\Big) &+ \boldsymbol{\Omega}\cdot\nabla\psi(\mathbf{x},E,\boldsymbol{\Omega},t) + \sigma_t(\mathbf{x},E,t)\psi(\mathbf{x},E,\boldsymbol{\Omega},t) \\
&= \int_{E'}\int_{4\pi}\sigma_s(\mathbf{x},E'{\to}E,\boldsymbol{\Omega}'{\to}\boldsymbol{\Omega},t)\psi(\mathbf{x},E',\boldsymbol{\Omega}',t)d\boldsymbol{\Omega}'dE' \\
&+\frac{\chi(E)}{4\pi}\int_{E'}\int_{4\pi}\bar{\nu}(E')\sigma_f(\mathbf{x},E',\boldsymbol{\Omega}',t)\psi(\mathbf{x},E',\boldsymbol{\Omega}',t)d\boldsymbol{\Omega}'dE' \\
&+q(\mathbf{x},E,\boldsymbol{\Omega},t)
\end{aligned}
\tag{1.5}
$$

To simplify the derivations, in the later parts of this text, we consider only the steady-state LBE

$$
\begin{aligned}
\boldsymbol{\Omega}\cdot\nabla\psi(\mathbf{x},E,\boldsymbol{\Omega}) + \sigma_t(\mathbf{x},E)\psi(\mathbf{x},E,\boldsymbol{\Omega}) &= \int_{E'}\int_{4\pi}\sigma_s(\mathbf{x},E'{\to}E,\boldsymbol{\Omega}'{\to}\boldsymbol{\Omega})\psi(\mathbf{x},E',\boldsymbol{\Omega}')d\boldsymbol{\Omega}'dE' \\
&+\frac{\chi(E)}{4\pi}\int_{E'}\int_{4\pi}\bar{\nu}(E')\sigma_f(\mathbf{x},E',\boldsymbol{\Omega}')\psi(\mathbf{x},E',\boldsymbol{\Omega}')d\boldsymbol{\Omega}'dE' \\
&+q(\mathbf{x},E,\boldsymbol{\Omega})
\end{aligned}
\tag{1.6}
$$

If we want to remove more complexity we can now drop the multiplication term (σ_f) to get the steady state **Linear Boltzmann Equation** in its most basic form,

$$
\Big(\boldsymbol{\Omega}\cdot\nabla + \sigma_t(\mathbf{x},E)\Big)\psi(\mathbf{x},E,\boldsymbol{\Omega}) = \int_{E'}\int_{4\pi}\sigma_s(\mathbf{x},E'{\to}E,\boldsymbol{\Omega}'{\to}\boldsymbol{\Omega})\psi(\mathbf{x},E',\boldsymbol{\Omega}')d\boldsymbol{\Omega}'dE' + q(\mathbf{x},E,\boldsymbol{\Omega}).
\tag{1.7}
$$

The equation above is in continuum form for all the independent variables $\mathbf{x}$, E, and $\mathbf{\Omega}$. The processes that follow are applied sequentially to this equation to arrive at a discretized system of equations that we can solve. The first process to apply is the multigroup approximation to remove the dependency on the continuous energy, also known as **energy discretization**. After that follows the removal of the angular dependence of the scattering terms, then the discretization of the angular domain (**angular discretization**) that ultimately results in the discrete ordinates formulation, and finally the application of a **spatial discretization** resulting in the fully discretized system to solve.

2 Multigroup approximation of the energy dependence

In order for us to remove the dependency on the discrete energy, which in many cases has a wide logarithmic range, we apply an energy discretization to reduce the continuous energy domain to a discrete group-based energy domain. There are several ways to formulate this energy discretization. As depicted in [1], we can use the separability of the group angular flux with a known function of energy. Alternatively, for more intuitive comprehension, we can use a more straight forward formulation that can be found in many texts. The text that follows will follow the latter approach.

We will refer to energy groups, in general, as they are defined in Figure 2.1 below.
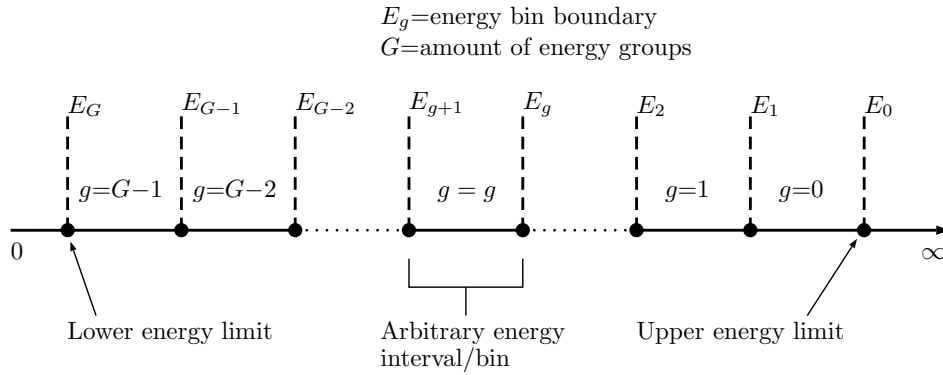
Figure 2.1: Definition of the energy groups as used by the code.

We start by defining intervals on the one dimensional energy domain that form our notion of a group. For a particular group we firstly require the definition of the group flux, ψ_g, which is the energy dependent flux integrated over the energy interval of a particular group. For this we have

$$\psi_g(\mathbf{x}, \mathbf{\Omega}) = \int_{E_{g+1}}^{E_g} \psi(\mathbf{x}, \mathbf{\Omega}, E) dE. \tag{2.1}$$

Next we seek to have a group cross section (for any type of interaction), σ_g, such that we preserve the continuous energy reaction rate. Therefore, we seek σ_g such that

$$\sigma_g(\mathbf{x})\psi_g(\mathbf{x}, \mathbf{\Omega}) = \int_{E_{g+1}}^{E_g} \sigma(\mathbf{x}, E)\psi(\mathbf{x}, \mathbf{\Omega}, E) dE \tag{2.2}$$

or in a more common notation

$$\sigma_g(\mathbf{x}) = \frac{\int_{E_{g+1}}^{E_g} \sigma(\mathbf{x}, E)\psi(\mathbf{x}, \mathbf{\Omega}, E) dE}{\int_{E_{g+1}}^{E_g} \psi(\mathbf{x}, \mathbf{\Omega}, E) dE}. \tag{2.3}$$

The major problem with this definition, however, is that we are developing multigroup cross sections for

the concise reason of determining the unknown $\psi(\mathbf{x}, \mathbf{\Omega}, E)$ (or an approximation thereof). So how could we possibly use the flux to compute these cross sections? The answer here is to replace the flux with a representative weighting spectrum, $w(E)$, such that

$$\sigma_g(\mathbf{x}) = \frac{\int_{E_{g+1}}^{E_g} \sigma(\mathbf{x}, E) w(E) dE}{\int_{E_{g+1}}^{E_g} w(E) dE}. \tag{2.4}$$

where w has the properties

$$w(E) \geq 0$$

$$\int_0^\infty w(E) dE = 1.$$

It is important to know that it is exceedingly important to choose the weighting function as close to to the spectrum, that will be observed in ψ, as possible. This is not always an easy task since it will be position dependent. Usually an initial estimation can be made with a constant weighting function.

In Figure 2.2 below an example is shown of a WIMS69 group structure applied to the incident-neutron total cross section, σ_t, of ^{14}N. The multigroup cross section is compared to the continuous energy cross section that generally spans a larger domain than that of the discrete.
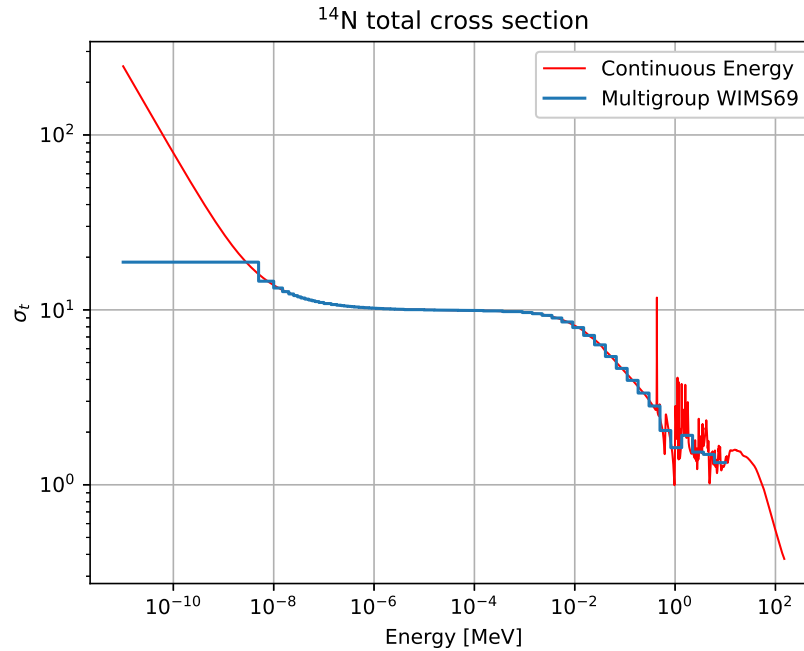
Figure 2.2: An example of a WIMS69 multigroup structure applied as an energy discretization of the total cross section of ^{14}N for neutron interactions. This is compared to continuous energy cross sections obtained from ENDF.

We now apply two modifications to eq. 1.7. Firstly we replace the integration over E' with a summation of integrals over the group intervals,

$$\int_{E'}\int_{4\pi}\sigma_s(\mathbf{x}, E'{\rightarrow}E, \boldsymbol{\Omega}'{\rightarrow}\boldsymbol{\Omega})\psi(\mathbf{x}, E', \boldsymbol{\Omega}')d\boldsymbol{\Omega}'dE' = \sum_{g'=0}^{G-1}\int_{E_{g'+1}}^{E_{g'}}\int_{4\pi}\sigma_s(\mathbf{x}, E'{\rightarrow}E, \boldsymbol{\Omega}'{\rightarrow}\boldsymbol{\Omega})\psi(\mathbf{x}, E', \boldsymbol{\Omega}')d\boldsymbol{\Omega}'dE',$$

secondly we integrate the entire equation over the energy interval of a particular group g,

$$\int_{E_{g+1}}^{E_g}\left(\boldsymbol{\Omega}{\cdot}\nabla + \sigma_t(\mathbf{x}, E)\right)\psi(\mathbf{x}, E, \boldsymbol{\Omega})dE$$

$$= \int_{E_{g+1}}^{E_g}\sum_{g'=0}^{G-1}\int_{E_{g'+1}}^{E_{g'}}\int_{4\pi}\sigma_s(\mathbf{x}, E'{\rightarrow}E, \boldsymbol{\Omega}'{\rightarrow}\boldsymbol{\Omega})\psi(\mathbf{x}, E', \boldsymbol{\Omega}')d\boldsymbol{\Omega}'dE'dE$$

$$+ \int_{E_{g+1}}^{E_g}q(\mathbf{x}, E, \boldsymbol{\Omega})dE,$$

for which we substitute our group quantities defined above to get the **multigroup Linear Boltzmann Equation**,

$$\left(\boldsymbol{\Omega}{\cdot}\nabla + \sigma_{tg}(\mathbf{x})\right)\psi_g(\mathbf{x}, \boldsymbol{\Omega}) = \sum_{g'=0}^{G-1}\int_{4\pi}\sigma_{s,g'{\rightarrow}g}(\mathbf{x}, \boldsymbol{\Omega}'{\rightarrow}\boldsymbol{\Omega})\psi_{g'}(\mathbf{x}, \boldsymbol{\Omega}')d\boldsymbol{\Omega}' + q_g(\mathbf{x}, \boldsymbol{\Omega}). \tag{2.5}$$

3 Expansion of angular functions

In a later section we will apply an angular discretization by which we can solve the LBE along discrete directions. The biggest challenge in this regard is the scattering from other angles and energies into a given angle-energy pair. From particle kinematics we can deduce that the probability of scattering from one discrete angle-energy pair to another discrete angle-energy pair assumes the nature of a δ-function, making it particularly hard to wield in numerical simulations.

With the introduction of the multigroup approximation we are at least offered the benefit of replacing the δ-functions with step-like functions for scattering between energy groups. This can be observed in Figure 3.1 which shows the nature of the step-like functions for a 5 group- and a 10 group scheme. The step-/ramp-like functions are formed because the scattering cosine, for scattering from one energy group g' to another group g, can span a range of cosine values dictated by the range of energies associated with groups g' and g.

The strategy of expanding these discontinuous step-like functions into reduced order bases effectively allows us to apply a Reduced Order Model (ROM) to the scattering process. With such a model only the expansion coefficients are computed, instead of the fully discretized angular domain, and essentially prevents the need to store the full angular flux (over all discrete directions) between iterations.

The choice of basis-functions for an expansion of an angular function arises mathematically from the spherical coordinate system naturally associated with the scattering angles. These basis functions are called the **Spherical Harmonic functions**. For an engineer the use of spherical harmonics will not be intuitive, but be assured that they are the appropriate choice. Another non-intuitive aspect is their relation to the well-known Legendre polynomials, to which they reduce when the angular expansion is for a function of the polar angle only.

In the sections that follow we first introduce the **Legendre expansion** for functions dependent only on the polar angle (actually the cosine of the polar angle $\mu = \cos\theta$) in a general sense. We then apply the general Legendre-expansion to the scattering interaction portion of the LBE in a section of its own. This is followed by a section on the Spherical Harmonics expansion for functions of both the polar- and azimuthal angles. Finally we replace relevant terms in the LBE with these expansions.
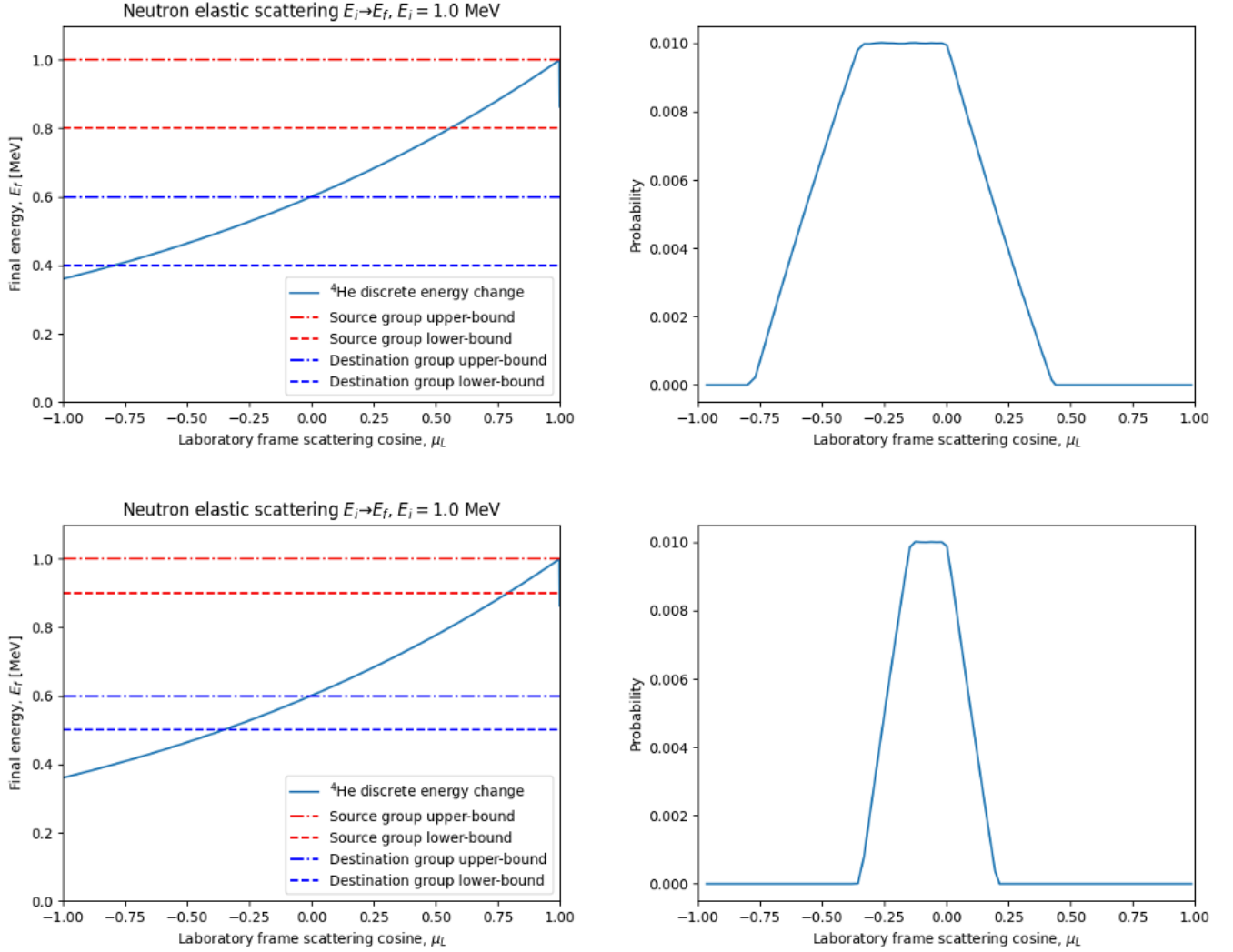
Figure 3.1: The two figures on the left shows the bounds of a source-group and a destination group, overlayed on the discrete energy change for a given cosine of scattering. The figures on the right shows the structure of the scattering kernel for multigroup probabilities. [Top-left] Shows the first and third group boundaries of a 5 group discretization. [Top-right] Shows a ramp-like function that is broad. [Bottom-left] Shows the first and fifth group boundaries for a 10 group discretization. [Bottom-right] Shows a ramp-like function that starts to narrow since the group of interest is narrower.

3.1 Legendre expansion of a function

This preface is required to understand our treatment of scattering cross-sections. It will not be clear immediately why this is done but please bear with the definitions. Using Legendre polynomials, any function $f(x)$, with x the single independent variable $\{x \in \mathbb{R} : -1 \leq x \leq 1\}$, can be represented exactly by the expansion f_{exp}, as

$$f(x) = f_{exp}(x) = \sum_{\ell=0}^{\infty} \frac{2\ell+1}{2} f_\ell \ P_\ell(x)$$

where the coefficients f_ℓ are defined by

$$f_\ell = \int_{-1}^{+1} f(x) \ P_\ell(x) dx.$$

This latter definition can create plenty of confusion since it depends on $f(x)$. Why then would we build an infinite series to represent a function $f(x)$ that we had in the first place? The first aspect to consider here is that we normally only build the expansion up to a certain order L (or truncation level) instead of ∞,

$$f(x) \approx \sum_{\ell=0}^{L} \frac{2\ell+1}{2} f_\ell \ P_\ell(x)$$

where the expansion becomes an approximation that is "good" enough for our purposes. The second aspect here, which will not become clear again until later, is the orthogonality properties that Legendre expansions have with regards to expansions using spherical harmonics.

As a preface the reader should note that for angular quantities dependent only on a single parameter, Legendre expansions are used whereas angular quantities dependent on both the polar and azimuthal angle, spherical harmonics expansions are used. The two expansions have orthogonality properties that we will exploit to simplify scattering between angles.

3.2   Legendre expansion of the scattering cross-section

The scattering cross-section of materials are normally available as a function of energy only. It is up to the user of the data to add the appropriate scattering kernels for which the scattering angles are a function of the masses of the neutron and its colliding nucleus as well as the energy. But first let us express the scattering terms in a Kernel fashion. We start with the scattering source term as is appears in equation 2.5,

$$\int_{4\pi} \sigma_{s,g' \to g}(\mathbf{x}, \mathbf{\Omega}' \to \mathbf{\Omega}) \psi_{g'}(\mathbf{x}, \mathbf{\Omega}') d\mathbf{\Omega}',$$

and recall the random scattering nature of neutral particles. In this regard it is important to note that two neutral particles interact in a reference frame that is somewhat arbitrary. Imagine for a moment that a particle is traveling along the x-axis in a cartesian reference frame and it collides with a target particle also on the x-axis that is stationary. The angle that the flight-path of the original particles now has with the x-axis can only be measured by the angle of the cone formed when rotating the reference frame around the x-axis. To this end we prefer to denote the scattering from $\mathbf{\Omega}' \to \mathbf{\Omega}$ with a cosine, μ. Therefore,

$$\int_{4\pi} \sigma_{s,g' \to g}(\mathbf{x}, \mathbf{\Omega}' \to \mathbf{\Omega}) \psi_{g'}(\mathbf{x}, \mathbf{\Omega}') d\mathbf{\Omega}' = 2\pi \int_{-1}^{+1} \sigma_{s,g' \to g}(\mathbf{x}, \mu) \psi_{g'}(\mathbf{x}, \mathbf{\Omega}') d\mathbf{\Omega}'$$

after which we apply a truncated Legendre expansion as

$$\sigma_{s,g'\rightarrow g}(\mathbf{x},\mu) \approx \sum_{\ell=0}^{L} \frac{2\ell+1}{4\pi}\sigma_{s\ell,g'\rightarrow g}(\mathbf{x})P_\ell(\mu) \tag{3.1}$$

where we used the 4π normalization to enable the expansion to appear in an integral over all angles. The scattering cross-section coefficients are normally determined outside the simulation, as inputs or material properties. An example of an expanded scattering cross section is shown in Figure 3.2 below.
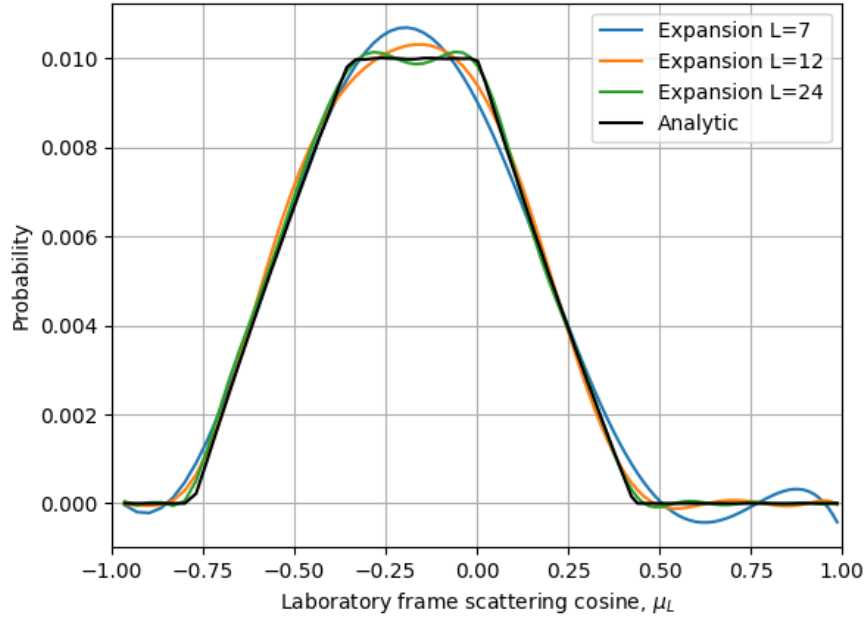
Figure 3.2: Example expansion of an angular cross section.

3.3 Spherical Harmonic expansion of angular functions

The entry point for a person researching spherical harmonics is inevitably the wikipedia and wolfram-alpha websites describing the complex valued spherical harmonics. From various sources it is evident that we can compute the same expansion by using the real forms of the sperical harmonics, called the **tesseral spherical harmonics**. This expansion is done in the form

$$f(\varphi,\theta) = \sum_{\ell=0}^{\infty} \sum_{m=-\ell}^{+\ell} \frac{2\ell+1}{4\pi}f_{\ell m}Y_{\ell m}(\varphi,\theta) \tag{3.2}$$

where

$$f_{\ell m} = \int_0^{2\pi} \int_0^{\pi} f(\varphi,\theta)Y_{\ell m}(\varphi,\theta)\sin\theta d\theta d\varphi$$

and

$$Y_{\ell m}(\theta, \varphi) = \begin{cases} (-1)^m \sqrt{(2)} \sqrt{\frac{(\ell-|m|)!}{(\ell+|m|)!}} P_\ell^{|m|}(\cos\theta) \sin|m|\varphi & \text{if } m < 0 \\ P_\ell^m(cos\theta) & \text{if } m = 0 \\ (-1)^m \sqrt{(2)} \sqrt{\frac{(\ell-m)!}{(\ell+m)!}} P_\ell^m(\cos\theta) \cos m\varphi & \text{if } m > 0 \end{cases}$$ (3.3)

Finally the polynomials, P_ℓ^m, called the **Associated Legendre Polynomials** are determined from

$$\begin{aligned} P_0^0 &= 1, \qquad P_1^0 = x, \\ P_\ell^\ell &= -(2\ell-1)\sqrt{1-x^2}\, P_{\ell-1}^{\ell-1}(x) \quad \text{and} \\ (\ell-m)P_\ell^m &= (2\ell-1)x\, P_{\ell-1}^m(x) - (\ell+m-1)P_{\ell-2}^m(x). \end{aligned}$$ (3.4)

It is important to note that from the basic definition of the associated Legendre Polynomials

$$P_\ell^m(x) = (-1)^m (1-x^2)^{m/2} \frac{d^m}{dx^m}(P_\ell(x))$$

we can see that the associated Legendre Polynomials equates to the ordinary Legendre Polynomials when $m = 0$. An additional property of this definition of the spherical harmonics, as opposed to the general definition found in literature (Wikipedia for example) is that when $\ell=0$, the first expansion coefficient is exactly the scalar flux. In equation-form the scalar flux is

$$\phi = \int_{4\pi} \psi(\mathbf{\Omega})d\mathbf{\Omega}$$

and from our definition

$$\begin{aligned} \phi_{00} &= \int_{4\pi} \psi(\mathbf{\Omega})Y_{00}(\mathbf{\Omega})d\mathbf{\Omega} \\ &= \int_{4\pi} \psi(\mathbf{\Omega})d\mathbf{\Omega}. \end{aligned}$$

Please also note that we will interchange a function $f(\varphi, \theta)$ with a function $f(\mathbf{\Omega})$ since the conversion between the two forms in either direction is known.

An example of a spherical harmonic expansion, of an analytic function, is shown in Figure 3.3 below.
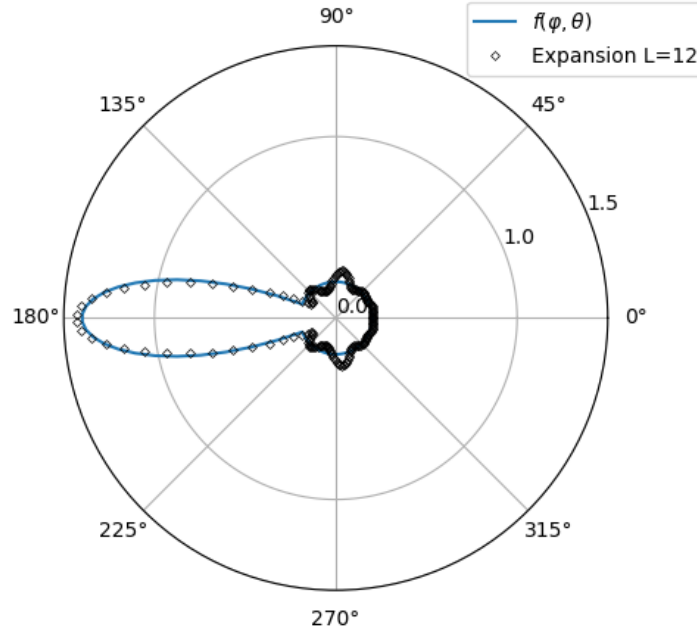
Figure 3.3: An example of a spherical harmonic expansion of an analytical function exhibiting a large degree of anisotropy. This plot is also shown in the appendices, where the related analytic function is detailed.

3.4 Spherical Harmonics expansion of the angular flux

We now approximate the angular flux, which appears in the scattering source, with a truncated expansion using spherical harmonics as

$$\psi(\mathbf{x}, E', \mathbf{\Omega}') \approx \sum_{\ell=0}^{L} \sum_{m=-\ell}^{+\ell} \frac{2\ell+1}{4\pi} \phi_{\ell m}(\mathbf{x}, E') Y_{\ell m}(\mathbf{\Omega}'), \tag{3.5}$$

where L is the truncation-level or order of the expansion, and

$$\phi_{\ell m}(\mathbf{x}, E') = \int_{4\pi} \psi(\mathbf{x}, E', \mathbf{\Omega}) \, Y_{\ell m}(\mathbf{\Omega}) \, d\mathbf{\Omega},$$

however, we never calculate $\phi_{\ell m}$ with this integral since ψ is still an unknown. Instead we calculate it from a set of linear equations as we will observe later. Now, if we plug equation 3.1 and 3.5 into equation 2.5 we get

$$\left(\mathbf{\Omega}\cdot\nabla+\sigma_{tg}(\mathbf{x})\right)\psi_g(\mathbf{x},\mathbf{\Omega})$$

$$= \sum_{g'=0}^{G-1}\int_{4\pi}\left[\sum_{\ell'=0}^{L}\frac{2\ell'+1}{4\pi}\sigma_{s\ell',g'\to g}(\mathbf{x})P_{\ell'}(\mu)\sum_{\ell=0}^{L}\sum_{m=-\ell}^{+\ell}\frac{2\ell+1}{4\pi}\phi_{g'\ell m}(\mathbf{x},E')Y_{\ell m}(\mathbf{\Omega}')d\mathbf{\Omega}'\right] \quad (3.6)$$

$$+ \; q_g(\mathbf{x},\mathbf{\Omega}).$$

If we only focus on the scattering term now, we first apply the addition theorem of spherical harmonics which states

$$P_\ell(\mu) = P_\ell(\mathbf{\Omega}'\cdot\mathbf{\Omega}) = \sum_{m=-\ell}^{\ell}Y_{\ell m}(\mathbf{\Omega})Y_{\ell m}(\mathbf{\Omega}'), \quad (3.7)$$

and if substituted into equation 3.6 gives

$$\left(\mathbf{\Omega}\cdot\nabla+\sigma_{tg}(\mathbf{x})\right)\psi_g(\mathbf{x},\mathbf{\Omega})$$

$$= \sum_{g'=0}^{G-1}\int_{4\pi}\left[\sum_{\ell'=0}^{L}\frac{2\ell'+1}{4\pi}\sigma_{s\ell',g'\to g}(\mathbf{x})\sum_{m'=-\ell'}^{\ell'}Y_{\ell'm'}(\mathbf{\Omega})Y_{\ell'm'}(\mathbf{\Omega}')\sum_{\ell=0}^{L}\sum_{m=-\ell}^{+\ell}\frac{2\ell+1}{4\pi}\phi_{g'\ell m}(\mathbf{x},E')Y_{\ell m}(\mathbf{\Omega}')d\mathbf{\Omega}'\right]$$

$$+ \; q_g(\mathbf{x},\mathbf{\Omega})$$

$$(3.8)$$

Now we can see numerous spherical harmonic functions multiplied together. However, they all appear inside an integral over all angle-space and therefore we can use the orthogonality of spherical harmonics from which follows

$$\int_{4\pi}Y_{\ell'm'}(\mathbf{\Omega}')Y_{\ell m}(\mathbf{\Omega}').d\mathbf{\Omega}' = \frac{4\pi}{2\ell'+1}\delta_{\ell\ell'}\delta_{mm'}, \quad (3.9)$$

and subsequently that all terms go to zero unless $\ell' = \ell$ and $m' = m$. When these conditions are met we then also replace the integral $\int_{4\pi}Y_{\ell'm'}(\mathbf{\Omega}')Y_{\ell m}(\mathbf{\Omega}').d\mathbf{\Omega}'$ with the expression above which reduces equation 3.8 to

$$\left(\mathbf{\Omega}\cdot\nabla+\sigma_{tg}(\mathbf{x})\right)\psi_g(\mathbf{x},\mathbf{\Omega}) = \sum_{g'=0}^{G-1}\sum_{\ell=0}^{L}\sum_{m=-\ell}^{\ell}\frac{2\ell+1}{4\pi}Y_{\ell m}(\mathbf{\Omega})\sigma_{s\ell,g'\to g}(\mathbf{x})\phi_{g'\ell m}(\mathbf{x}) \; + \; q_g(\mathbf{x},\mathbf{\Omega}). \quad (3.10)$$

where we re-arrange the loop over energy groups for efficiency purposes as

$$\left(\mathbf{\Omega}\cdot\nabla+\sigma_{tg}(\mathbf{x})\right)\psi_g(\mathbf{x},\mathbf{\Omega}) = \sum_{\ell=0}^{L}\sum_{m=-\ell}^{\ell}\frac{2\ell+1}{4\pi}Y_{\ell m}(\mathbf{\Omega})\sum_{g'=0}^{G-1}\sigma_{s\ell,g'\to g}(\mathbf{x})\phi_{g'\ell m}(\mathbf{x}) \; + \; q_g(\mathbf{x},\mathbf{\Omega}). \quad (3.11)$$

4 The Discrete Ordinates Method (S_N Method)

Recall that an angular function expanded using real spherical harmonics is denoted as

$$f(\theta, \varphi) = \sum_{\ell=0}^{\infty} \sum_{m=-\ell}^{\ell} \frac{2\ell+1}{4\pi} f_{\ell m} Y_{\ell m}(\theta, \varphi),$$

where

$$f_{\ell m} = \int_0^\pi \int_0^{2\pi} f(\theta, \varphi) Y_{\ell m}(\theta, \varphi) \sin\theta d\theta d\varphi$$

Similarly,

$$\phi_{g\ell m}(\mathbf{x}) = \int_{4\pi} \psi_g(\mathbf{x}, \mathbf{\Omega}) Y_{\ell m}(\mathbf{\Omega}) d\mathbf{\Omega}.$$

The fundamental approach of the Discrete Ordinates Method is to approximate this integral with a **quadrature rule** such that

$$\int_{4\pi} \psi_g(\mathbf{x}, \mathbf{\Omega}) Y_{\ell m}(\mathbf{\Omega}).d\mathbf{\Omega} \approx \sum_{n=0}^{N} w_n \ \psi_g(\mathbf{x}, \mathbf{\Omega}_n) Y_{\ell m}(\mathbf{\Omega}_n),$$

or with an index on the angular flux, $\psi_g(\mathbf{x}, \mathbf{\Omega}_n) = \psi_{gn}(\mathbf{x})$,

$$\int_{4\pi} \psi_g(\mathbf{x}, \mathbf{\Omega}) Y_{\ell m}(\mathbf{\Omega}).d\mathbf{\Omega} \approx \sum_{n=0}^{N} w_n \ \psi_{gn}(\mathbf{x}) Y_{\ell m}(\mathbf{\Omega}_n), \tag{4.1}$$

Where the weights w_n and associated directions $\mathbf{\Omega}_n$ are particular to the quadrature rule (or rule set) used, and for a particular direction $\mathbf{\Omega}_n$ we then write $\psi_g(\mathbf{x}, \mathbf{\Omega}_n) = \psi_{gn}(\mathbf{x})$.

The multi-group LBE (i.e. equation 2.5) now becomes the angular neutron transport equation

$$\left(\mathbf{\Omega}_n \cdot \nabla + \sigma_{tg}(\mathbf{x})\right) \psi_{gn}(\mathbf{x}) = \sum_{\ell=0}^{\infty} \sum_{m=-\ell}^{\ell} \frac{2\ell+1}{4\pi} Y_{\ell m}(\mathbf{\Omega}_n) \left[\sum_{g'=0}^{G-1} \sigma_{s\ell, g' \to g}(\mathbf{x}) \phi_{g'\ell m}(\mathbf{x}) \right] + q_{gn}(\mathbf{x}). \tag{4.2}$$

After then plugging the above angular quadrature-rule into equation 4.2 we get

$$\left(\mathbf{\Omega}_n \cdot \nabla + \sigma_{tg}(\mathbf{x})\right) \psi_{gn}(\mathbf{x}) = \sum_{\ell=0}^{\infty} \sum_{m=-\ell}^{\ell} \frac{2\ell+1}{4\pi} Y_{\ell m}(\mathbf{\Omega}_n) \left[\sum_{g'=0}^{G-1} \sigma_{s\ell, g' \to g}(\mathbf{x}) \left(\sum_{n'=0}^{N} w_{n'} Y_{\ell m}(\mathbf{\Omega}_{n'}) \psi_{g'n'}(\mathbf{x}) \right) \right] + q_{gn}(\mathbf{x}). \tag{4.3}$$

4.1 Remapping the moment indices

At this point it is necessary to think about how to solve this problem. The indices of the spherical harmonics ($Y_{\ell m}$) is bothersome since it is not one dimensional but fortunately we can remap them. Let us suppose we have the regular spherical harmonics $Y_{l m^*}$ and we propose Y_m with only one index such that $(\ell, m^*) \rightarrow m$. For example, in three dimensions we will have the following

$$
\begin{aligned}
&\text{when } \ell = 0, \quad Y_0 = Y_{0,0} \\
&\text{when } \ell = 1, \quad Y_1 = Y_{1,-1} \quad Y_2 = Y_{1,0} \quad Y_3 = Y_{1,1} \\
&\text{when } \ell = 2, \quad Y_4 = Y_{2,-2} \quad Y_5 = Y_{2,-1} \quad Y_6 = Y_{2,0} \quad Y_7 = Y_{2,1} \quad Y_8 = Y_{2,2} \\
&\qquad\qquad\qquad\qquad\qquad \vdots
\end{aligned}
$$

and so forth.

The maximum index m per ℓ follows the sequence

$$
\begin{array}{ccccc}
\ell = 0 & \ell = 1 & \ell = 2 & \ldots & \ell = L \\
0 & 0+(2+1) & 0+(2+1)+(4+1) & \ldots & 0+(2+1)+(4+1)+\ldots+(2L+1)
\end{array}
\tag{4.4}
$$

which can be expressed as a series that has the form

$$
m_{max} = \sum_{\ell=1}^{L} (2\ell+1),
\tag{4.5}
$$

but when expanded in a forward and backward sense such that

$$
\sum_{\ell=1}^{L} (2\ell+1) = (2+1)+(4+1)+(6+1)+\ldots+(2(L-1)+1)+(2L+1)
$$

$$
\text{and } \sum_{\ell=1}^{L} (2\ell+1) = (2L+1)+(2(L-1)+1))+\ldots+(6+1)+(4+1)+(2+1),
$$

we can observe a pattern when adding these sequences together:

$$
2\sum_{\ell=1}^{L} (2\ell+1) = (2L+4)+(2L+4)+\ldots+(2L+4)+(2L+4)+(2L+4)
$$

$$
= L(2L+4)
$$

Therefore this series reduces to

$$
m_{max} = L(L+2)
\tag{4.6}
$$

Therefore the maximum m-index for a given ℓ is $\ell(\ell+2)$ and corresponds to $m^* = +\ell$. This leads us to the definition of the mapping

$$
\{(\ell, m^*) \rightarrow m : m = \ell(\ell+2)+m^*-\ell\}
$$

which is also graphically depicted below in Figure 4.1.

L\m	-5	-4	-3	-2	-1	0	1	2	3	4	5
0						0					
1					1	2	3				
2				4	5	6	7	8			
3			9	10	11	12	13	14	15		
4		16	17	18	19	20	21	22	23	24	
5	25	26	27	28	29	30	31	32	33	34	35

Figure 4.1: Indices of Y_m as a subset of $Y_{\ell m^*}$ for three dimensional geometry.

We can also find the number of moments, N_{moms}, associated with any L. Within this formulation $N_{moms} = m_{max}+1$ which simplifies to

$$N_{moms} = L^2+2L+1 = (L+1)^2 \tag{4.7}$$

with the inverse mapping $N_{moms} \rightarrow L$ easily obtained from

$$L = \sqrt{N_{moms}} - 1 \tag{4.8}$$

Specialization for 2D cartesian coordinates

For a 2D function, where the angular flux is not a function of θ, the angular integrals to determine the $\phi_{\ell m}$ coefficients evaluate to zero on certain indices. For each ℓ the set of non-zero coefficients have indices in accordance with

$$m = \begin{cases} 0 & \text{if } \ell = 0 \\ -1, +1 & \text{if } \ell = 1 \\ -2, +2 & \text{if } \ell = 2 \\ -3, -1, +1, +3 & \text{if } \ell = 3 \\ -4, -2, +2, +4 & \text{if } \ell = 4 \\ -\ell, -\ell+2, -\ell+4, ..., \ell & m \neq 0, \text{ if } \ell > 4 \end{cases} \tag{4.9}$$

Graphically this is depicted in Figure 4.2 below.

L\m	-5	-4	-3	-2	-1	0	1	2	3	4	5
0						0					
1					1		2				
2				3				4			
3			5		6		7		8		
4		9		10				11		12	
5	13		14		15		16		17		18

Figure 4.2: Indices of Y_m as a subset of $Y_{\ell m^*}$ for two dimensional geometry.

Finding the number of moments is not as easy as for the 3D or 1D case, regardless we can find this value from

$$N_{moms} = 2 \left\lfloor \frac{L}{2} \right\rfloor \left(\left\lfloor \frac{L}{2} \right\rfloor + 1 \right) + 2 \bmod \left(\frac{L}{2} \right) \left\lceil \frac{L}{2} \right\rceil + 1. \tag{4.10}$$

The inverse mapping $N_{moms} \to L$ can be obtained from

$$L = 2C_1 + \frac{C_2}{\max(1, C_2)} \tag{4.11}$$

where

$$C_1 = \left\lfloor -\frac{1}{4} + \frac{1}{2}\sqrt{1 + 2(N_{moms} - 1)} \right\rfloor$$

$$C_2 = N_{moms} - 1 - 2C_1 - 2C_1^2.$$

Specialization for 1D cartesian coordinates

For a 1D angular flux the spherical harmonic expansions reduce to Legendre expansions and hence only the ℓ, m indices where $m = 0$ are considered. Hence:

$$N_{moms} = L + 1 \tag{4.12}$$

Graphically this is depicted in Figure 4.3 below.

L\m	-5	-4	-3	-2	-1	0	1	2	3	4	5
0						0					
1						1					
2						2					
3						3					
4						4					
5						5					

Figure 4.3: Indices of Y_m as a subset of $Y_{\ell m^*}$ for one dimensional geometry.

4.2 The multigroup Discrete Ordinates Equation

With the re-indexing defined in section 4.1 we can recast equation 4.3 to get the **Discrete Ordinates Equation**,

$$\left(\mathbf{\Omega}_n \cdot \nabla + \sigma_{tg}(\mathbf{x}) \right) \psi_{gn}(\mathbf{x}) = \sum_{m=0}^{m_{max}} \frac{2\ell+1}{4\pi} Y_{\ell m^*}(\mathbf{\Omega}_n) \sum_{g'=0}^{G-1} \left[\sigma_{sm,g' \to g}(\mathbf{x}) . \phi_{mg'}(\mathbf{x}) \right] + q_{g,n}(\mathbf{x}) \tag{4.13}$$

where ℓ and m^* is mapped from m. This form then serves our discussion for the development of the operator form of the LBE.

5 Application of the Discontinuous Galerkin Finite Element Method

To comprehend the application of the DG-FEM spatial discretization to our previous formulations we consider a simplified version of the fundamental equations above, namely

$$\Omega \cdot \nabla \psi + \sigma \psi = q \tag{5.1}$$

where we dropped the direction index n and the group index g, however, this equation needs to be solved for each group g and each angle n. For each node in the spatial discretization we multiply by the (not yet defined) trial space τ_i and require that

$$\int_V \left[\tau_i \Omega \cdot \nabla \psi + \sigma \tau_i \psi - \tau_i q \right] \, dV = 0.$$

$$\int_V \tau_i \Omega \cdot \nabla \psi \, dV + \int_V \sigma \tau_i \psi \, dV - \int_V \tau_i q \, dV = 0. \tag{5.2}$$

Applying integration by parts to the first term results in

$$\int_V \Omega \cdot \nabla (\tau_i \psi) \, dV - \int_V \psi \Omega \cdot \nabla \tau_i \, dV + \int_V \sigma \tau_i \psi \, dV - \int_V \tau_i q \, dV = 0 \tag{5.3}$$

where we can apply Gauss's divergence theorem to the first term to obtain

$$\int_{\partial V} (\Omega \cdot \mathbf{n}) \tau_i \psi \, dS - \int_V \psi \Omega \cdot \nabla \tau_i \, dV + \int_V \sigma \tau_i \psi \, dV - \int_V \tau_i q \, dV = 0. \tag{5.4}$$

We now apply an upwinding scheme to the boundary integral

$$\int_{\partial V} (\Omega \cdot \mathbf{n}) \tau_i \tilde{\psi} \, dS - \int_V \psi \Omega \cdot \nabla \tau_i \, dV + \int_V \sigma \tau_i \psi \, dV - \int_V \tau_i q \, dV = 0.$$

where

$$\tilde{\psi} = \begin{cases} \psi_{withincell} & \text{if } \mathbf{n} \cdot \Omega > 0 \\ \psi_{upwindcell} & \text{if } \mathbf{n} \cdot \Omega < 0 \end{cases} \tag{5.5}$$

At this juncture the finite element weak-form is complete enough for us to use. The boundary integral can be split into separate faces and we can assemble a system on a cell-by-cell basis provided that the upstream fluxes are known.

5.1 Second-order elements

For the case where non-curved elements are used there is a simplification we can make to these equations that will negate the requirement to loop over all faces to compute the surface integral and instead only loop over faces that have incident angular fluxes (i.e., $\mathbf{\Omega} \cdot \mathbf{n}_f < 0$). This is done as follows:

We again apply integration by parts to the second term in the equation above,

$$\int_{\partial V} (\Omega \cdot \mathbf{n}) \tau_i \tilde{\psi} \ dS - \int_V \Omega \cdot \nabla(\tau_i \psi) \ dV + \int_V \tau_i \Omega \cdot \nabla \psi \ dV + \int_V \sigma \tau_i \psi \ dV - \int_V \tau_i q \ dV = 0.$$

and then Gauss's divergence theorem again on the second term,

$$\int_{\partial V} (\Omega \cdot \mathbf{n}) \tau_i (\tilde{\psi} - \psi) \ dS + \int_V \tau_i \Omega \cdot \nabla \psi \ dV + \int_V \sigma \tau_i \psi \ dV - \int_V \tau_i q \ dV = 0.$$

From this equation we can see that the boundary integration, over faces that are not incident, will cancel to zero since the upstream flux is the same as the internal flux.

Now, when we expand ψ and $\tilde{\psi}$ into basis functions, as

$$\psi = \sum_{j=0}^{j_{max}} b_j \psi_j \text{ and } \tilde{\psi} = \sum_{j=0}^{j_{max}} b_j \tilde{\psi}_j$$

we arrive at the "per DOF" version of the finite element equation

$$\sum_{j=0}^{j_{max}} \left[\int_{\partial V} (\Omega \cdot \mathbf{n}) \tau_i (\tilde{\psi}_j b_j - \psi_j b_j) \ dS + \int_V \psi_j \tau_i \Omega \cdot \nabla b_j \ dV + \int_V \sigma \psi_j \tau_i b_j \ dV \right] = \sum_{j=0}^{j_{max}} \int_V \tau_i q_j b_j \ dV. \tag{5.6}$$

Note we also expanded the source term q. From this equation we see that we need expressions for the shape function τ_i and b_j as well as the derivative of the trial function gradient $\nabla \tau_i$. We also need a means to efficiently integrate these functions over surface and volume. With a Galerkin finite element method the trial space function τ_i and the basis functions b_i are the same functions so that the above equation reduces to

$$\sum_{j=0}^{j_{max}} \left[\int_{\partial V} (\Omega \cdot \mathbf{n}) b_i b_j \ dS \ (\tilde{\psi}_j - \psi_j) + \Omega \cdot \int_V b_i \nabla b_j \ dV \ \psi_j + \sigma \int_V b_i b_j \ dV \ \psi_j \right] = \sum_{j=0}^{j_{max}} \int_V b_i b_j \ dV \ q_j. \tag{5.7}$$

For second order elements we can associate an average normal, $\mathbf{n}$, with each face and therefore evaluation of the surface integral will be consistent across a face given the upwinding condition. This allows the precomputation of all the integrals in these equations as

$$\int_{\partial V} (\Omega \cdot \mathbf{n}) b_i b_j \ dS = \sum_{\substack{f=0 \\ \Omega \cdot \mathbf{n}_f < 0}}^{f_{max}} (\Omega \cdot \mathbf{n}_f) M_{cf,ij}$$

$$M_{cf,ij} = \int_f b_i b_j \ dS$$

$$M_{c,ij} = \int_V b_i b_j \ dV$$

$$G_{c,ij} = \int_V b_i \nabla b_j \ dV$$

using quadrature rules. Each of these ij entries for a cell c then combine into cell-matrices, M_{cf} with entries $M_{cf,ij}$ (also called the cell-face mass-matrix), M_c with entries $M_{c,ij}$ (also called the cell mass-matrix), and finally G_c with entries $G_{c,ij}$ (also called the cell gradient-matrix). We can also define the nodal angular flux vectors for cell c as $\boldsymbol{\psi}_c = [\psi_0, \ldots, \psi_{N_{nodes,c}}]$ and $\tilde{\boldsymbol{\psi}}_{c,f} = [\tilde{\psi}_0, \ldots, \tilde{\psi}_{N_{nodes,c}}]$ for the upstream fluxes at face f, where $N_{nodes,c}$ is the number of nodes on cell c. Similarly we also define the angular source vector $\mathbf{q}_c^{\Omega} = [q_0, \ldots, q_{N_{nodes,c}}]$. Applying these matrices to the weak formulation above, and noting $(\boldsymbol{\Omega} \cdot \mathbf{n}_f) = \mu_f$, we get the system

$$\boldsymbol{\Omega} \cdot G_c \boldsymbol{\psi}_c + \sigma M_c \boldsymbol{\psi}_c - \sum_{\substack{f=0 \\ \mu_f < 0}}^{f_{max}} \mu_f M_{cf} \boldsymbol{\psi}_c + \sum_{\substack{f=0 \\ \mu_f < 0}}^{f_{max}} \mu_f M_{cf} \tilde{\boldsymbol{\psi}}_c = M_c \mathbf{q}_c^{\Omega}$$

$$\left(\boldsymbol{\Omega} \cdot G_c + \sigma M_c + \sum_{\substack{f=0 \\ \mu_f < 0}}^{f_{max}} \mu_f M_{cf} \right) \boldsymbol{\psi}_c + \left(\sum_{\substack{f=0 \\ \mu_f < 0}}^{f_{max}} \mu_f M_{cf} \tilde{\boldsymbol{\psi}}_{c,f} \right) = M_c \mathbf{q}_c^{\Omega}.$$

(5.9)

When all $\tilde{\boldsymbol{\psi}}_{c,f}$ are known, the system essentially reduces to

$$A_c \boldsymbol{\psi}_c = \mathbf{b}_c,$$

where

$$A_c = \boldsymbol{\Omega} \cdot G_c + \sigma M_c + \sum_{\substack{f=0 \\ \mu_f < 0}}^{f_{max}} \mu_f M_{cf}$$

and

$$\mathbf{b}_c = M_c \mathbf{q}_c^{\Omega} - \left(\sum_{\substack{f=0 \\ \mu_f < 0}}^{f_{max}} \mu_f M_{cf} \tilde{\boldsymbol{\psi}}_{c,f} \right)$$

which can be solved using Gaussian-elimination without pivoting. Gaussian elimination is chosen because the size of the A_c matrix to invert is fairly small, i.e., 2×2 for a 1D slab, 4×4 for a 2D quadrilateral and up to 22×22 for a 3D polyhedron, with a high probability of always being smaller than 100×100.

5.2 Perspective of each cell-by-cell system relative to all cells

Each cell-by-cell system requires $\tilde{\boldsymbol{\psi}}_c$ which is only available from the cells upstream. For discussion purposes we can now resume the notations that include the direction index n and the group index g, and define a contiguous vector $\boldsymbol{\psi}_{gn}$ holding all the nodal angular fluxes for a particular direction, for all cell-nodes in the domain and also an accompanying angular source $\mathbf{b}_{gn}$ (constructed from individual $M_c \mathbf{q}_c$ pieces). We now also define a re-indexing of cells, with index symbol $c \in [0, N_{cells})$, according to their **topographical order** (w.r.t. direction n). Let us then define an upstream cell c', with c' belonging to the set of cell indices

pointing to cells upstream of cell c. With these definitions in place the system above can be rewritten as a collection of individual matrices

$$A_{cc}\boldsymbol{\psi}_{gn} + \sum_{c'} A_{cc'}\boldsymbol{\psi}_{gn} = \mathbf{b}_{gn}$$

where each matrix A_{ij} is a single-entry block matrix (i.e., only the ij block has an entry). For example

$$A_{cc} = \begin{bmatrix} 0 & \cdots & & \cdots & & \cdots & 0 \\ \vdots & \ddots & & & & & \vdots \\ \vdots & & A_{cc}^{entry} & & & \vdots \\ \vdots & & & & \ddots & & \vdots \\ 0 & \cdots & & \cdots & & \cdots & 0 \end{bmatrix} \qquad A_{cc'} = \begin{bmatrix} 0 & \cdots & & \cdots & \cdots & 0 \\ \vdots & \ddots & & & & \vdots \\ \vdots & A_{cc'}^{entry} & 0 & & & \vdots \\ \vdots & & & & \ddots & \vdots \\ 0 & \cdots & & \cdots & \cdots & 0 \end{bmatrix}$$

Each of the single-entry matrices can be added to a block matrix L_{gn} with block dimension $(N_{cells}-1)\times(N_{cells}-1)$. Now, if each index c is guaranteed to be downstream from all associated c' then when the individual single-entry matrices are assembled into the L_{gn} block-matrix then the resulting matrix is a block lower-triangular matrix. Note that this is highly dependent on the existence of an actual topographical sorting, which requires the absence of cyclic dependencies, however, for now we will use the classical denotation of this block lower-triangular matrix being denoted as L_{gn} and forms the system

$$L_{gn}\boldsymbol{\psi}_{gn} = \mathbf{b}_{gn}$$

with dimension $N_{nodes}\times N_{nodes}$.

6 Operator form of the discretized Linear Boltzmann equation

In later sections, where we define algorithms for solving the discretized LBE, we require the definition of several operators. Firstly we need the **transport operator L**. Then, to convert flux-moments (ϕ_m) to discrete angular fluxes (ψ), we need the **moment-to-discrete operator, M**. To perform the opposite conversion, where angular fluxes are converted to flux-moments, we need the **discrete-to-moment operator, D**. We also need the **scattering operator, S**, to hold the operator relating to scattering. Following the M, D and S operators we simply have the external source vector Q.

The structure of each of these operators is highly dependent on the structure of ϕ, the vector of flux-moments over all moments, groups and nodes. For example, ϕ can be stacked in any of the orders; group-moment-node, group-node-moment, moment-node-group, moment-group-node, node-group-moment and node-moment-group. For purposes of comprehensively combining the transport operator with other operators we will depict the structure as a **group-moment-node structure for ϕ**. Similarly we also have a **group-direction-node structure for ψ**.

Note that none of the operators, that are defined in the subsections that follow, **are ever built or stored as a whole matrix** since at the most fundamental level **they are nested block matrices** for which we only need to define the most fundamental block.

6.1 The transport operator

The system $L_{gn}\psi_{gn} = \mathbf{b}_{gn}$, for direction n and group g, defined in the finite element spatial discretization, can be expanded as follows. First we define an angle-consolidated block matrix L^{Ω} for group g as

$$L_g^{\Omega} = \mathrm{diag}(\ L_{g0}, \ldots, L_{gn_{max}}\ )^{N_{dirs} \times N_{dirs}}$$

which has a block dimension $N_{dirs} \times N_{dirs}$ and a discrete dimension $(N_{nodes}N_{dirs}) \times (N_{nodes}N_{dirs})$. We then assemble these matrices for each group g into the matrix L as

$$L = \mathrm{diag}(\ L_0^{\Omega}, \ldots, L_{g_{max}}^{\Omega}\ )^{G \times G}$$

which has block dimension $G \times G$ and discrete dimension $(N_{nodes}N_{dirs}G) \times (N_{nodes}N_{dirs}G)$ and is compatible with the ψ vector.

6.2 Definition of the moment-to-discrete operator, M

After altering equation 4.13 we have

$$\left(\mathbf{\Omega}_n \cdot \nabla + \sigma_{tg}(\mathbf{x})\right)\psi_{gn}(\mathbf{x}) = \sum_{m=0}^{m_{max}} M_{nm}^{nodal} \sum_{g'=0}^{G}\left[\sigma_{sm,g'\to g}(\mathbf{x}).\phi_{mg'}(\mathbf{x})\right] + q_{g,n}(\mathbf{x}) \tag{6.1}$$

where M_{nm}^{nodal} is an entry in the matrix M^{nodal} and forms the fundamental matrix-block needed to develop M. The entries are

$$M_{nm}^{nodal} = \frac{2\ell+1}{4\pi} Y_{\ell m^*}(\mathbf{\Omega}_n) \tag{6.2}$$

where ℓ and m^* are mapped from m. This matrix is known as the **nodal moment-to-discrete operator** since it is the same on each node of the problem and converts a vector of moment quantities (at a given g index and node) to a vector of angular quantities. In other words, given the moment vector $\boldsymbol{\phi}_{i,g}$ where each entry is a flux moment $\phi_{i,g,m}$ at node i for group g, the nodal matrix allows the conversion

$$\boldsymbol{\psi}_{i,g} = M^{nodal} \boldsymbol{\phi}_{i,g}$$

where each entry $\psi_{i,g,n}$ is the angular flux at node i, for group g and direction n.

A structure for the eventual M-operator, which is compatible with $\boldsymbol{\phi}$ and $\boldsymbol{\psi}$, is defined as follows. First we define a block matrix M^Ω for any group g as

$$M^\Omega : \text{ entries } M_{nm}^\Omega = \text{diag}(\ M_{nm}^{nodal}, \ldots, M_{nm}^{nodal}\ )^{N_{nodes} \times N_{nodes}}.$$

which has block dimension $N_{dirs} \times N_{moms}$ and discrete dimension $(N_{dirs} N_{nodes}) \times (N_{moms} N_{nodes})$. This block matrix is then used to define the operator M as

$$M = \text{diag}(\ M^\Omega, \ldots, M^\Omega\ )^{G \times G}$$

with each entry the same (i.e., M^Ω). This operator has block dimension $G \times G$ and discrete dimension $(G \times N_{dirs} \times N_{nodes}) \times (G \times N_{moms} \times N_{nodes})$ and therefore allows the conversion

$$\boldsymbol{\psi} = M\boldsymbol{\phi}.$$

6.3   Definition of the discrete-to-moment operator, D

Similar to the way the moment-to-discrete operator used the re-indexing of moments we can use this re-indexing in the quadrature rule for determining each element $\phi_{mg'}$, where

$$\phi_{mg'} = \sum_{n'=0}^{N} w_{n'} Y_m(\mathbf{\Omega}_n') \psi_{g'n'}(\mathbf{x})$$

$$= \sum_{n'=0}^{N} D_m(\mathbf{\Omega}_n) \psi_{g'n'}(\mathbf{x}).$$

where D_m is developed from each ℓ, m^* pair and angle index n to get

$$D_m(\mathbf{\Omega}_n) = D_{mn}^{nodal} = w_{n'} Y_m(\mathbf{\Omega}_n') \tag{6.3}$$

The latter D^{nodal}-matrix with D_{mn}^{nodal} entries, is known as the **nodal discrete-to-moment operator** since it is the same on each node of the problem and converts a vector of angular quantities (at a given g index and node) to a vector of moment quantities.

A structure for the eventual D-operator, which is compatible with ϕ and ψ, is defined as follows. First we define a block matrix D^Ω for any group g as

$$D^\Omega : \text{with entries } D_{mn}^\Omega = \text{diag}(\ D_{mn}^{nodal}, \ldots, D_{mn}^{nodal}\ )^{N_{nodes} \times N_{nodes}}.$$

This matrix has block dimension $N_{moms} \times N_{dirs}$ and discrete dimension $(N_{moms} N_{nodes}) \times (N_{dirs} N_{nodes})$ and is then nested into the D-operator as

$$D = \text{diag}(\ D^\Omega, \ldots, D^\Omega\ )^{G \times G}$$

which then has a discrete dimension $(G N_{moms} N_{nodes}) \times (G N_{dirs} N_{nodes})$ and therefore allows the conversion

$$\phi = D\psi.$$

6.4 The external source vector, Q

The external source vector is comprised of a number of nested vector. The first level involves the application of the cell mass-matrix M_c to get the vector

$$Q_{gnc} = M_c \mathbf{q}_c^\Omega$$

which has discrete dimension $N_{nodes,c} \times 1$ and is nested into the cell-consolidated vector

$$Q_{gn} = [Q_{gn0}, \ldots, Q_{gnN_{cells}}]$$

which has block dimension $N_{cells} \times 1$ and discrete dimension $N_{nodes} \times 1$. This vector is then nested into the angle-consolidated vector

$$Q_g = [Q_{g0}, \ldots, Q_{gn_{max}}]$$

which has block dimension $N_{dirs} \times 1$ and discrete dimension $(N_{dirs} N_{nodes} \times 1$. This vector is then finally assembled into

$$Q = [Q_0, \ldots, Q_{g_{max}}]$$

which has block dimension $G \times 1$ and discrete dimension $G N_{dirs} N_{nodes} \times 1$.

6.5 The final operator form

Combining all the operators defined above we get the form

$$L\psi = MSD\psi + Q \tag{6.4}$$

7 Algorithms

7.1 Source Iteration or Classic Richardson iteration

Source iteration involves an initial scattering source $MSD\boldsymbol{\psi}^{(0)}$ after which each $\boldsymbol{\psi}$ is determined from the iterative algorithm depicted by

$$\boldsymbol{\psi}^{(k+1)} = L^{-1}MSD\boldsymbol{\psi}^{(k)} + L^{-1}Q. \tag{7.1}$$

Some manipulations to this algorithm can, however, afford us some benefit. One such manipulation originates from the observation that the dimension of the flux-moment vector $\boldsymbol{\phi}$ is often orders of magnitude less than that of the angular flux vector $\boldsymbol{\psi}$ and therefore it would be beneficial if algorithms can selectively only store $\boldsymbol{\phi}$. If we multiply the above equation by the D-operator we get

$$D\boldsymbol{\psi}^{(k+1)} = DL^{-1}MSD\boldsymbol{\psi}^{(k)} + DL^{-1}Q.$$

after which we can note the fact that $D\boldsymbol{\psi} = \boldsymbol{\phi}$ to get

$$\boldsymbol{\phi}^{(k+1)} = DL^{-1}MS\boldsymbol{\phi}^{(k)} + DL^{-1}Q. \tag{7.2}$$

This equation then allows us to perform iterations on $\boldsymbol{\phi}$ only and therefore requires significantly less storage than the equivalent algorithm iterating on $\boldsymbol{\psi}$.

7.2 Krylov subspace methods - GMRES

If we reformulate the operator form to contain only known quantities on the right-hand side then we can assemble an $A\mathbf{x} = \mathbf{b}$ form of the problem. To do this we do not lag the scattering source and now perform the following manipulations

$$L\boldsymbol{\psi} = MSD\boldsymbol{\psi} + Q$$
$$L\boldsymbol{\psi} - MSD\boldsymbol{\psi} = Q$$
$$(L - MSD)\boldsymbol{\psi} = Q$$
$$L^{-1}(L - MSD)\boldsymbol{\psi} = L^{-1}Q$$
$$(I - L^{-1}MSD)\boldsymbol{\psi} = L^{-1}Q$$

and, similar to the Source Iteration algorithm, we can multiply with the D operator to then finally get

$$\underbrace{(I - DL^{-1}MS)}_{A} \underbrace{\boldsymbol{\phi}}_{\mathbf{x}} = \underbrace{DL^{-1}Q}_{\mathbf{b}}. \tag{7.3}$$

This equation has two algorithmic portions to it. The first is the $DL^{-1}Q$ called the "Compute b" portion and the second is the $(I - DL^{-1}MS)\mathbf{v}$ portion called the "Operator action" where the action of the matrix-A on a Krylov-vector $\mathbf{v}$. These two portions form the basis of the GMRES algorithm.

Appendix A   Quadrature rules for integration over angle-space

Suppose we have a function of azimuthal angle φ and polar angle θ namely, $f(\varphi, \theta)$, and we integrate this function over the entire angular domain. We seek a quadrature rule (or a combination of rules) that will allow the simplified integration in the form

$$\int_0^{2\pi} \int_0^{\pi} f(\varphi, \theta) \sin \theta d\theta d\varphi \approx \sum_n^N w_n f((\varphi, \theta)_n).$$

Here the values w_n are weights and $(\varphi, \theta)_n$ are the abscissae of the t.b.d. quadrature rule. However, the form of this integral is not yet in a form conducive to the application of quadrature rules. To this end we observe that

$$\mu = \cos \theta$$

and

$$\frac{d\mu}{d\theta} = - \sin \theta$$

We can now express f as a function of μ instead of θ for which we have

$$\int_0^{2\pi} \int_1^{-1} -f(\varphi, \mu) d\mu d\varphi$$
$$= \int_0^{2\pi} \int_{-1}^{1} f(\varphi, \mu) d\mu d\varphi$$

This equation is convenient since we can apply quadrature rules to each angular case. To see this let us assign

$$g(\varphi) = \int_{-1}^{1} f(\varphi, \mu) d\mu \tag{A.1}$$

for which we now have

$$\int_0^{2\pi} g(\varphi) d\varphi. \tag{A.2}$$

A.1   Gauss-Legendre quadrature rule

The *Gauss-Legendre* quadrature rule is used when the weighting function is unity, i.e. $w(x){=}1$, and therefore we can integrate the function in the form

$$\int_{-1}^{1} f(x) dx \approx \sum_{n=1}^{N} w_n f(x_n).$$

Here the abscissae x_n are the roots of the Legendre polynomial $P_n(x)$, and the weights are

$$w_n = \frac{2(1-x_n^2)}{(n+1)^2(P_{n+1}(x_n))^2} \tag{A.3}$$

From this equation we can see we need to evaluate the values of the Legendre polynomials. For this purpose we use the recursion of Legendre polynomials stating that

$$
\begin{aligned}
P_0(x) &= 1 \\
P_1(x) &= x \\
P_{n+1}(x) &= \left(\frac{2n+1}{n+1}\right)xP_n(x) - \left(\frac{n}{n+1}\right)P_{n-1}(x)
\end{aligned}
\tag{A.4}
$$

Using the code below these functions can be evaluated.

```python
def Legendre(N,x):
    Pnm1 = 1;
    Pn   = x;
    Pnp1 = 0;

    if (N==0):
        return 1;

    if (N==1):
        return x;

    for n in range(2,N+1):
        ns=n-1
        Pnp1 = ((2*ns+1)/(ns+1))*x*Pn -(ns/(ns+1))*Pnm1;
        Pnm1 = Pn;
        Pn = Pnp1;

    return Pnp1
```

The other unknown in equation A.3 is the abscissae x_n which are the roots of the Legendre polynomial equations. An algorithm for finding these roots is given by Barrerra-Figueroa [2]. This algorithm utilizes Newton's method for finding a root and therefore we need to also have a function for finding the derivate of the Legendre polynomials

$$P_n'(x) = \frac{nx}{x^2-1}P_n(x) - \frac{n}{x^2-1}P_{n-1}(x) \tag{A.5}$$

The code below obtains the derivative $P_n'(x)$:

```python
def dLegendredx(N,x):
    if (N==0):
        return 0;

    if (N==1):
        return 1;

    return (N*x/(math.pow(x,2)-1))*Legendre(N,x)- \
            (N/(math.pow(x,2)-1))*Legendre(N-1,x);
```

Finally applying the root finding equation in [2]

$$x_k^{(\ell+1)} = x_k^{(\ell)} - \frac{f(x_k^{(\ell)})}{f'(x_k^{(\ell)}) - f(x_k^{(\ell)}) \sum_{j=1}^{k-1} \frac{1}{x_k^{(\ell)} - x_j}} \tag{A.6}$$

We get the code

```python
def LegendreRoots(N,maxiters=1000,tol=1.0e-10):
    xn = np.linspace(-0.999,0.999,N);  #Initial guessed values

    print("Initial guess:")
    print(xn)

    wn = np.zeros((N));


    for k in range(0,N):
        print("Finding root %d of %d" % (k+1,N), end='')
        i=0;
        while (i<maxiters):
            xold = xn[k]
            a = Legendre(N,xold)
            b = dLegendredx(N,xold)
            c = 0;
            for j in range(0,k):
                c=c+(1/(xold-xn[j]))

            xnew = xold - (a/(b-a*c))

            res=abs(xnew-xold)
            xn[k]=xnew

            if (res<tol):
                print('tr',end='')
                break
            i=i+1

        wn[k] = 2*(1-xn[k]*xn[k])/(N+1)/(N+1)/ \
                Legendre(N+1,xn[k])/Legendre(N+1,xn[k])
        print(" root %f, weight=%f, test=%f" %(xn[k],wn[k],Legendre(N,xn[k])))

    return xn,wn;
```

With the result for $P_5(x)$:

```
Finding root 1 of 5 root1 -0.906180, weight=0.236927

Finding root 2 of 5 root1 -0.538469, weight=0.478629

Finding root 3 of 5 root1 0.000000, weight=0.568889

Finding root 4 of 5 root1 0.538469, weight=0.478629

Finding root 5 of 5 root1 0.906180, weight=0.236927
```

A.2 Gauss-Chebyshev quadrature rule

The *Gauss-Chebyshev* quadrature rule is used when the weighting is $w(x) = \frac{1}{\sqrt{1-x^2}}$ and therefore the integral is of the form

$$\int_{-1}^{1} \frac{f(x)}{\sqrt{1-x^2}} dx \approx \sum_{n=1}^{N} w_n f(x_n).$$

Here the abscissae x_n are the roots of the Chebyshev polynomials of the second kind which have an explicit solution:

$$x_n = \cos\left(\frac{(2n-1)\pi}{2N}\right). \tag{A.7}$$

The quadrature weights are given by the simple relation

$$w_n = \frac{\pi}{N}. \tag{A.8}$$

The code below is a simple implementation of these formulas

```
def ChebyshevRoots(N):
    xn = np.linspace(-1,1,N)
    wn = np.linspace(-1,1,N)

    for n in range(0,N):
        ns=n+1
        xn[n]=math.cos((2*ns-1)*math.pi/2/N)
        wn[n]=math.pi/N

        print("Finding root %d of %d, root=%f, weight=%f" %(n+1,N,xn[n],wn[n]))

    return xn,wn
```

With the result for $U_5(x)$:

```
Finding root 1 of 5, root=0.951057, weight=0.628319

Finding root 2 of 5, root=0.587785, weight=0.628319

Finding root 3 of 5, root=0.000000, weight=0.628319

Finding root 4 of 5, root=-0.587785, weight=0.628319

Finding root 5 of 5, root=-0.951057, weight=0.628319
```

A.3   Application to Discrete Ordinates

We can find the polar angles associated with the polar quadrature directly from our earlier definition

$$g(\varphi) = \int_{-1}^{1} f(\varphi, \mu) d\mu \approx \sum_{i=0}^{2N_p-1} w_i f(\varphi, \mu_i)$$

where N_p is the number of polar quadrature points/angles in the first octant. The abscissae μ_i are obtained from the roots of the Legendre polynomial P_{2N_p} and the weights are

$$w_i = \frac{2(1-\mu_i^2)}{(i+2)^2 (P_{i+2}(\mu_i))^2}. \tag{A.9}$$

The angles associated with the abscissae are then

$$\theta_i = cos^{-1}\mu_i \tag{A.10}$$

A.4   Gauss-Legendre-Legendre product quadrature

The integration over all azimuthal angles requires some thought. In its defined form

$$\int_0^{2\pi} g(\varphi) d\varphi.$$

it can utilize the Gauss-Legendre quadrature after a change of intervals from $[0, 2\pi]$ to $[-1, 1]$ as

$$\int_0^{2\pi} g(\varphi) d\varphi = \frac{2\pi-0}{2} \int_{-1}^{1} g(\frac{2\pi-0}{2}y + \frac{2\pi+0}{2}) dy$$

$$= \pi \int_{-1}^{1} g(\pi y + \pi) dy$$

$$\approx \sum_{j=0}^{4N_a-1} w_j g(\pi y_j + \pi)$$

where again N_a is the amount of azimuthal angles per octant and the quadrature points are the abscissae of the Legendre polynomial P_{4N_a} and the weights are

$$w_j = \frac{2\pi(1-y_j^2)}{(j+2)^2 (P_{j+2}(y_j))^2}. \tag{A.11}$$

The angles associated with the abscissae are then

$$\varphi_j = \pi y_j + \pi \tag{A.12}$$

and we now have a product quadrature of the form

$$\int_0^{2\pi} \int_0^{\pi} f(\varphi, \theta) \sin\theta d\theta d\varphi \approx \sum_{j=0}^{4N_a-1} w_j \left[\sum_{i=0}^{2N_p-1} w_i f(\varphi_j, \theta_i) \right]. \tag{A.13}$$

An example of this quadrature is shown for the first octant in Figure A1.1 where the colors and dot size indicate the quadrature weight and the dot's position indicates the quadrature point on the unit sphere.
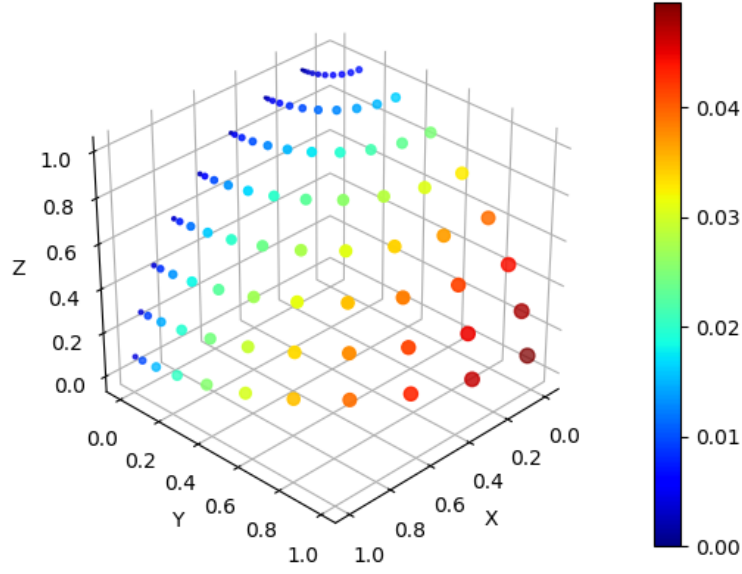

Figure A1.1: Quadrature points and weights (colors) for the Gauss-Legendre quadrature set for both the polar and azimuthal angles with $N_a = 8$ and $N_p = 8$.

A.5 Gauss-Legendre-Chebyshev product quadrature

Instead of changing the intervals of the integration over the azimuthal angles φ we can instead look towards utilizing these intervals by defining

$$y = \cos(\frac{\varphi}{2})$$

and

$$\frac{dy}{d\varphi} = -\frac{1}{2}\sin(\frac{\varphi}{2}).$$

Therefore

$$d\varphi = -\frac{2}{\sin(\frac{\varphi}{2})}.dy$$

$$= -\frac{2}{\sqrt{1-\cos^2(\frac{\varphi}{2})}}dy$$

$$\therefore d\varphi = -\frac{2}{\sqrt{1-y^2}}dy$$

which can be used in equation A.2 as

$$\int_0^{2\pi} g(\varphi)d\varphi = \int_1^{-1} -2\frac{g(2\cos^{-1}y)}{\sqrt{1-y^2}}dy$$

$$= 2\int_{-1}^1 \frac{g(2\cos^{-1}y)}{\sqrt{1-y^2}}dy$$

and when we define, for simplicity, $h(y) = g(2\cos^{-1}y)$ we get a familiar form

$$\int_0^{2\pi} g(\varphi)d\varphi = 2\int_{-1}^1 \frac{h(y)}{\sqrt{1-y^2}}dy. \tag{A.14}$$

This equation can be approximated with a Gauss-Chebyshev quadrature with abscissae

$$y_j = \cos\left(\frac{(2j+1)\pi}{8N_a}\right) \tag{A.15}$$

and equal weights

$$w_j = \frac{2\pi}{4N_a} \tag{A.16}$$

where N_a is the number of quadrature points per octant, to get the quadrature formula

$$\int_{-1}^1 \frac{h(y)}{\sqrt{1-y^2}}dy \approx \sum_{j=0}^{4N_a-1} w_j h(y_j). \tag{A.17}$$

The angles associated with the abscissae are then

$$\varphi_j = \frac{(2j+1)\pi}{8N_a} \tag{A.18}$$

and we now have a product quadrature of the form

$$\int_0^{2\pi} \int_0^{\pi} f(\varphi, \theta) \sin \theta d\theta d\varphi \approx \sum_{j=0}^{4N_a-1} w_j \left[\sum_{i=0}^{2N_p-1} w_i f(\varphi_j, \theta_i) \right]. \tag{A.19}$$

An example of this quadrature is shown for the first octant in Figure A1.2 where the colors and dot size indicate the quadrature weight and the dot's position indicates the quadrature point on the unit sphere.
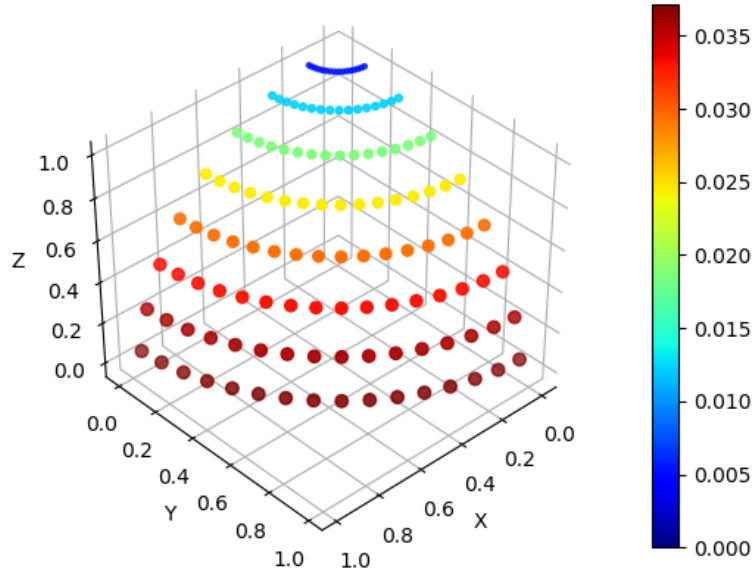

Figure A1.2: Quadrature points and weights (colors) for the Gauss-Legendre quadrature for the polar integration and the Gauss-Chebyshev quadrature for the azimuthal angles with $N_a = 8$ and $N_p = 8$.

A.6 Evaluation of product quadratures

With the quadrature candidates established we can now look at their performance. The application of the product quadratures is done to calculate the integral

$$\int_{4\pi} \psi_g(\mathbf{x}, \mathbf{\Omega}) Y_{\ell m^*}(\mathbf{\Omega}) d\mathbf{\Omega}$$

where the angular flux $\psi(\mathbf{x}, \mathbf{\Omega})$ is known at the point where the integration is to be performed. Hence we are essentially looking for a function to integrate the spherical harmonic $Y_{lm^*}(\mathbf{\Omega})$ where, repeated here

$$Y_{\ell m*}(\theta, \varphi) = (-1)^m Y_{\ell(-m)}(\theta, \varphi)$$

$$Y_{\ell m}(\theta, \varphi) = \begin{cases} (-1)^m \sqrt{(2)} \sqrt{\frac{(2\ell+1)}{4\pi} \frac{(\ell-|m|)!}{(\ell+|m|)!}} P_\ell^{|m|}(\cos\theta) \sin |m|\varphi & \text{if } m < 0 \\ (-1)^m \sqrt{(2)} \sqrt{\frac{(2\ell+1)}{4\pi} \frac{(\ell-m)!}{(\ell+m)!}} P_\ell^m(\cos\theta) \cos m\varphi & \text{if } m \geq 0 \end{cases} \tag{A.20}$$

where the associated Legendre polynomials, P_ℓ^m can be determined from

$$P_0^0 = 1, \qquad P_1^0 = x,$$
$$P_\ell^\ell = -(2\ell-1)\sqrt{1-x^2} \, P_{\ell-1}^{\ell-1}(x) \quad \text{and} \tag{A.21}$$
$$(\ell-m)P_\ell^m = (2\ell-1)x \, P_{\ell-1}^m(x) - (\ell+m-1)P_{\ell-2}^m(x).$$

An algorithm implementation to evaluate these associated Legendre polynomials is shown below.

```python
def AssociatedLegendre(ell,m,x):
    if (abs(m)>ell):
        return 0;

    #      m=0,l=1
    Pn    = x;

    #      m=1,l=1
    Pnpos= -math.sqrt(1-math.pow(x,2));
    #      m=-1,l=1
    Pnneg= -0.5*Pnpos;

    #      m=0,l=0
    if (ell==0):
        return 1;

    if (ell==1):
        if (m==-1):
            return Pnneg;
        if (m==0):
            return Pn;
        if (m==1):
            return Pnpos;

    Pmlp1 = 0
    if (ell==m):
        Pmlp1 = -(2*ell-1)*math.sqrt(1-math.pow(x,2.0))* \
                AssociatedLegendre(ell-1,ell-1,x)
```

```
    else:
        Pmlp1 = (2*ell-1)*x*AssociatedLegendre(ell-1,m,x);
        Pmlp1 = Pmlp1 - (ell+m-1)*AssociatedLegendre(ell-2,m,x)
        Pmlp1 = Pmlp1 / (ell-m)

    return Pmlp1
```

An algorithm implementation of the tesseral spherical harmonics is shown below.

```
#----------------------------------
def fac(x):
    if (x==0):
        return 1
    if (x==1):
        return 1

    return fac(x-1)*x;

#----------------------------------
def Min1powerm(m):
    if (m==0):
        return 1;
    if ((m%2)==0):
        return 1
    else:
        return -1

#----------------------------------
def Ylm(ell,m,theta,varphi):
    if (m<0):
        return Min1powerm(m)*math.sqrt( \
                ( (2*ell+1)/(2*math.pi) )* \
                fac(ell-abs(m))/fac(ell+abs(m)) )* \
                AssociatedLegendre(ell,abs(m),math.cos(theta))* \
                math.sin(abs(m)*varphi)
    else:
        return Min1powerm(m)*math.sqrt( \
                ( (2*ell+1)/(2*math.pi) )* \
                fac(ell-m)/fac(ell+m) )* \
                AssociatedLegendre(ell,m,math.cos(theta))* \
                math.cos(m*varphi)
```

Appendix B More on Spherical Harmonics

B.1 Expansion of a function of two angles $f(\varphi, \theta)$, Wikipedia flavor

We seek to expand an angularly dependent function $f(\theta, \varphi)$. Why? Don't know yet, but one such expansion from fundamental theory is spherical harmonics:

$$f(\theta, \varphi) = \sum_{\ell=0}^{\infty} \sum_{m=-\ell}^{\ell} f_\ell^m Y_\ell^m(\theta, \varphi). \tag{B.1}$$

This expansion will be very unfamiliar for engineers since most of the scientific computing in common disciplines deal with cartesian coordinates. Also, searches ultimately route to the complex versions such as those found on Wikipedia, adding to the confusion. Unfortunately it will be nearly impossible to explain the development of an expansion of an angular function in spherical harmonics without first exploring the means to calculate its unknowns. To this end let us begin with stating that **there are two flavors of spherical harmonics**. The regular form Y_ℓ^m, which contains complex numbers (challenging to handle), and a real form $Y_{\ell m}$. The unknowns in equation B.1 has a trail of components the first of which is

$$\begin{aligned} f_\ell^m &= \int_{\mathbf{\Omega}} f(\theta, \varphi) \, Y_\ell^{m^*}(\theta, \varphi) \, d\mathbf{\Omega} \\ &= \int_0^{2\pi} \int_0^{\pi} f(\theta, \varphi) Y_\ell^{m^*}(\theta, \varphi) \sin\theta d\theta d\varphi. \end{aligned}$$

The reader should try to comprehend that the f_ℓ^m components are almost never computed in this form since doing so means one already has an analytical representation of $f(\theta, \varphi)$. Additionally we have

$$Y_\ell^m(\theta, \varphi) = \sqrt{\frac{(2\ell+1)}{4\pi} \frac{(\ell-m)!}{(\ell+m)!}} \cdot P_\ell^m(\cos\theta) e^{(m\varphi)i} \tag{B.2}$$

This form of the spherical harmonics functions can be very unruly and therefore its more common place to calculate them from the real forms as

$$Y_\ell^m(\theta, \varphi) = \begin{cases} \frac{1}{\sqrt{2}}(Y_{\ell|m|} - iY_{\ell, -|m|}) & \text{if } m < 0 \\ Y_{\ell 0} & \text{if } m = 0 \\ \frac{(-1)^m}{\sqrt{2}}(Y_{\ell|m|} + iY_{\ell, -|m|}) & \text{if } m > 0 \end{cases} \tag{B.3}$$

Here the real forms are represented by:

$$Y_{\ell m}(\theta, \varphi) = \begin{cases} (-1)^m \sqrt{2}\sqrt{\frac{(2\ell+1)}{4\pi} \frac{(\ell-|m|)!}{(\ell+|m|)!}} P_\ell^{|m|}(\cos\theta) \sin\,|m|\varphi & \text{if } m < 0 \\ \sqrt{\frac{(2\ell+1)}{4\pi}} P_\ell^m & \\ (-1)^m \sqrt{2}\sqrt{\frac{(2\ell+1)}{4\pi} \frac{(\ell-m)!}{(\ell+m)!}} P_\ell^m(\cos\theta) \cos\,m\varphi & \text{if } m \geq 0 \end{cases} \tag{B.4}$$

Finally the associated Legendre polynomials, P_ℓ^m can be determined from

$$P_0^0 = 1, \qquad P_1^0 = x,$$
$$P_\ell^\ell = -(2\ell-1)\sqrt{1-x^2}\, P_{\ell-1}^{\ell-1}(x) \quad \text{and} \tag{B.5}$$
$$(\ell-m)P_\ell^m = (2\ell-1)x\, P_{\ell-1}^m(x) - (\ell+m-1)P_{\ell-2}^m(x).$$

With all these unknowns we see that before we can calculate the expansion we need to choose the maximum order $L = \ell_{max}$ after which we need to compute each P_ℓ^m, each $Y_{\ell m}$, each Y_ℓ^m and each $Y_\ell^{m^*}$. Only then can we compute f_ℓ^m. If we do all the work this way we can approximate some functions.

B.2 The more practical form of spherical harmonic expansions

The wikipedia version of a spherical harmonic expansion shows the basic properties of the expansion very well, however, in practice we employ a slight modification of the harmonics circumventing the complex mathematics entirely. Firstly, we remove the $\sqrt{\dfrac{2\ell+1}{4\pi}}$-factor out of equation (B.4) to get

$$Y_{\ell m}(\theta, \varphi) = \begin{cases} (-1)^m \sqrt{2}\sqrt{\frac{(\ell-|m|)!}{(\ell+|m|)!}} P_\ell^{|m|}(\cos\theta)\sin\,|m|\varphi & \text{if } m < 0 \\ P_\ell^m(\cos\theta) & \\ (-1)^m \sqrt{2}\sqrt{\frac{(\ell-m)!}{(\ell+m)!}} P_\ell^m(\cos\theta)\cos\,m\varphi & \text{if } m \geq 0 \end{cases} \tag{B.6}$$

Secondly, we account for the removal of this term by defining a spherical harmonic expansion as

$$f(\varphi, \theta) = \sum_{\ell=0}^{\infty} \sum_{m=-\ell}^{\ell} \frac{2\ell+1}{4\pi} f_{\ell m} Y_{\ell m}(\varphi, \theta) \tag{B.7}$$

where

$$f_{\ell m} = \int_0^{2\pi} \int_0^{\pi} f(\varphi, \theta) Y_{\ell m}(\varphi, \theta) \sin\theta d\theta d\varphi.$$

Benefits of this form:
The primary benefit of formulating the spherical harmonics in this form is that the expansion coefficients take on familiar forms when used to expand angular flux quantities. For instance, if $f(\varphi, \theta) \to \psi(\varphi, \theta)$, and $f_{\ell m} \to \phi_{\ell m}$, then

$$\phi_{00} = \int_0^{2\pi} \int_0^{\pi} \psi(\varphi, \theta) Y_{\ell m}(\varphi, \theta) \sin\theta d\theta d\varphi$$
$$= \int_{4\pi} \psi(\mathbf{\Omega}) Y_{\ell m}(\mathbf{\Omega}) d\mathbf{\Omega}.$$

This makes **the zeroth moment equivalent to the scalar flux** which is beneficial for use with the scattering cross sections. This form of the spherical harmonics also satisfy all the desirable properties of the complex counterpart. It satisfies the orthogonality property previously stated in 3.9 and repeated here

$$\int_{4\pi} Y_{l'm'}(\boldsymbol{\Omega'})Y_{\ell m}(\boldsymbol{\Omega'}).d\boldsymbol{\Omega} = \frac{4\pi}{2\ell'+1}\delta_{ll'}\delta_{mm'}, \tag{B.8}$$

and it lends itself to the addition theorem used in equation 3.7

$$P_\ell(\cos\theta_s) = P_\ell(\boldsymbol{\Omega'}\cdot\boldsymbol{\Omega}) = \sum_{m=-\ell}^{\ell} Y_{\ell m}(\boldsymbol{\Omega})Y_{\ell m}(\boldsymbol{\Omega'}). \tag{B.9}$$

B.3   Testing the angular expansion nature of Sperical harmonics

We can test the ability to expand angular functions into spherical harmonics by applying the expansion to known angular functions. Suppose we have any function of angle F.

B.3.1   Approximating an isotropic flux

The simplest function to represent is an isotropic flux (i.e. $f(\varphi,\theta) = 1$). Such a function is perfectly captured with $L = 0$, i.e. a single expansion, as shown in Figure B2.1.
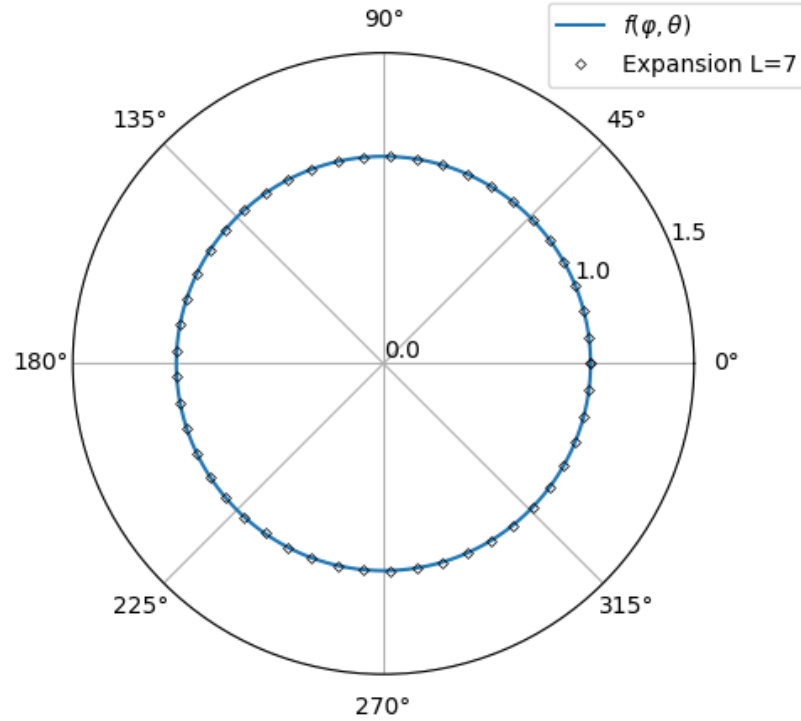
```
def F0(varphi,theta):
    return 1
```

Figure B2.1: Approximation of a pure isotropic function with spherical harmonics. The plot is shown for the azimuthal angle φ only.

B.3.2 Approximating an anisotropic but smooth flux

We can construct an anisotropic function of azimuthal angle as

$$f(\varphi, \theta) = 1+0.1*\cos(4\varphi)$$

```
def F1(varphi,theta):
    return 1.0+0.1*math.cos(varphi*4)
```

Such a function requires a few more orders of spherical harmonics in order to capture the shape and, as shown in Figure B2.2, $L = 7$ closely resembles the shape. A function of this shape could appear in a fuel assembly lattice where the effective scattering and absorbtion is a strong function of azimuthal angle.
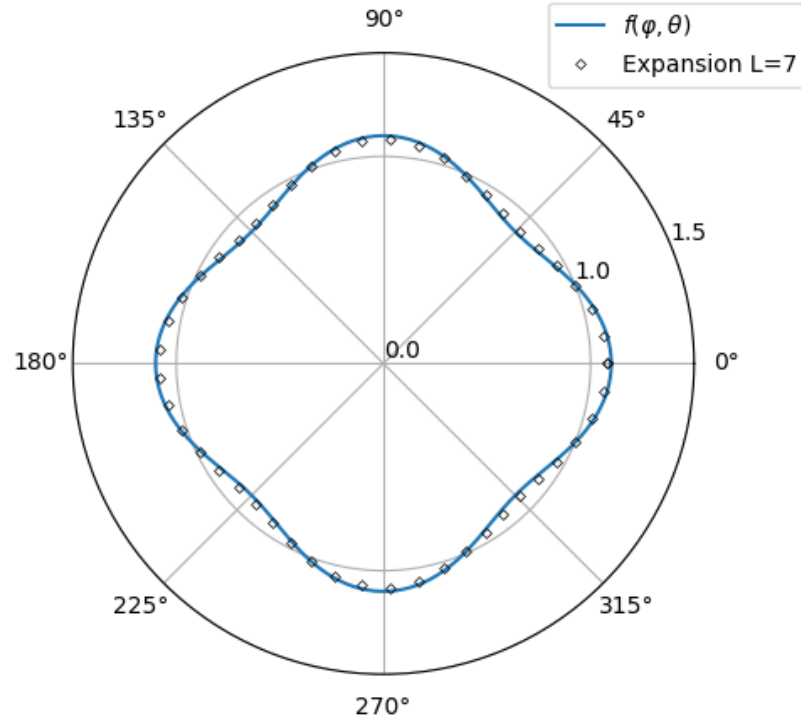
Figure B2.2: Approximation of an anisotropic smooth function with spherical harmonics. The plot is shown for the azimuthal angle φ only. The radial dimension represents the flux magnitude.

B.3.3 Approximating a directional flux (i.e. anisotropic + not-smooth)

As a final consideration we try to construct a function that is very angular, like a beam. Such a function of angle could be

$$f(\varphi, \theta) = \begin{cases} \frac{2}{10} & \text{if} \quad \varphi < \frac{7}{8}\pi \\ \frac{2}{10} + \frac{6}{5}\cos(4\varphi) & \text{if} \quad \frac{7}{8}\pi \leq \varphi \leq \frac{9}{8}\pi \\ \frac{2}{10} & \text{if} \quad \varphi > \frac{9}{8}\pi \end{cases}$$

```
def F2(varphi,theta):
    if (varphi<(7*math.pi/8)):
        return 0.2;
    if (varphi>(9*math.pi/8)):
        return 0.2;

    return 1.2*math.cos(varphi*4)+0.2
```

As expected a total number of 12 spherical harmonic orders are required to accurately represent such a directional flux (see Figure B2.3). An additional 2D plot is shown in Figure B2.4 which more clearly shows the oscillations of the expansion at the directions not aligned with the directional nature of the function.
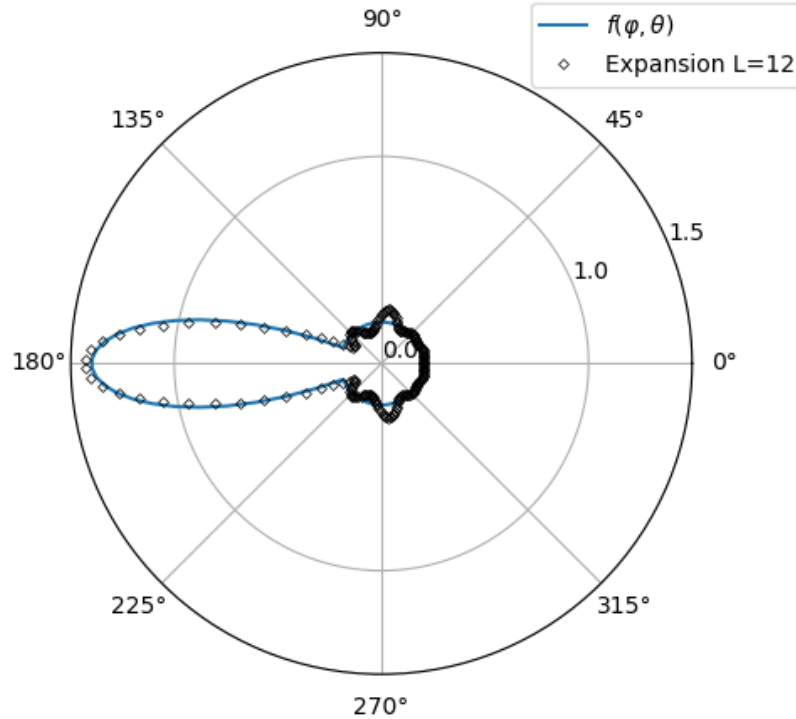

Figure B2.3: Approximation of an anisotropic non-smooth function with spherical harmonics. The plot is shown for the azimuthal angle φ only. The radial dimension represents the flux magnitude.
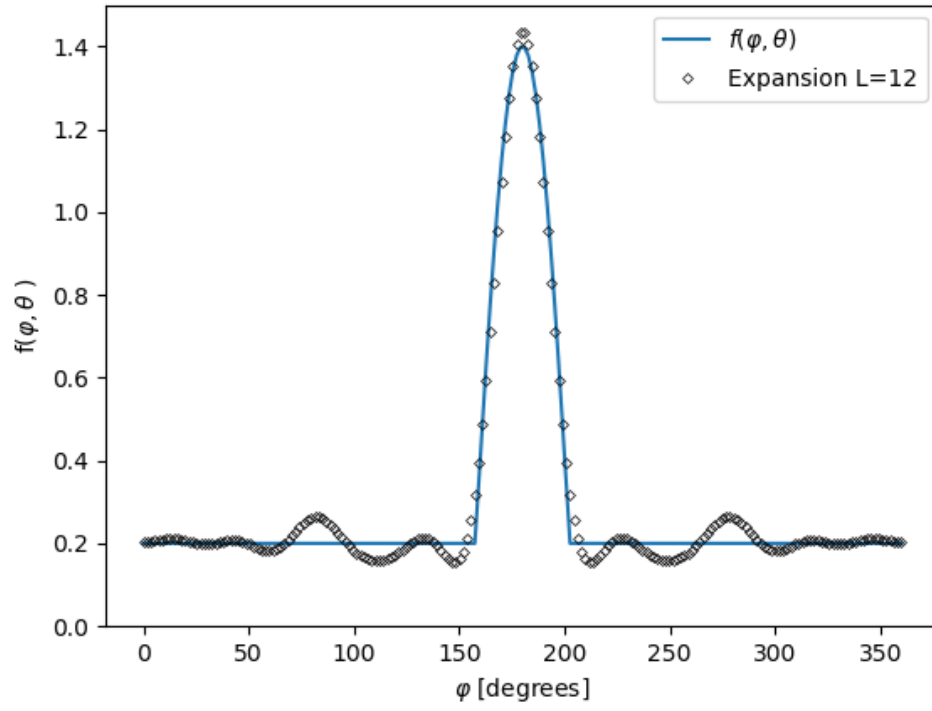
Figure B2.4: Approximation of an anisotropic non-smooth function with spherical harmonics. The plot is shown for the azimuthal angle φ only.

Appendix C Creating simple materials for testing anisotropic scattering

Neutral particle transport involves three basic processes:

- Absorption. The elimination of the particle from a current group

- Scattering. Change in angle and group essentially removing the particle from the group-angle pair.

- Source. Both in the form of a fixed source and as reactions to absorption processes (i.e. (n,n), (n,2n), (n,fission), etc.)

We also have a fundamental definition that the total removal process is the sum of the absorption process and the scattering process. In terms of nuclide cross-sections we can write this as

$$\sigma_t = \sigma_a + \sigma_s$$

Where σ_t, σ_a and σ_s represent the total-, absorption- and scattering cross-sections respectively.

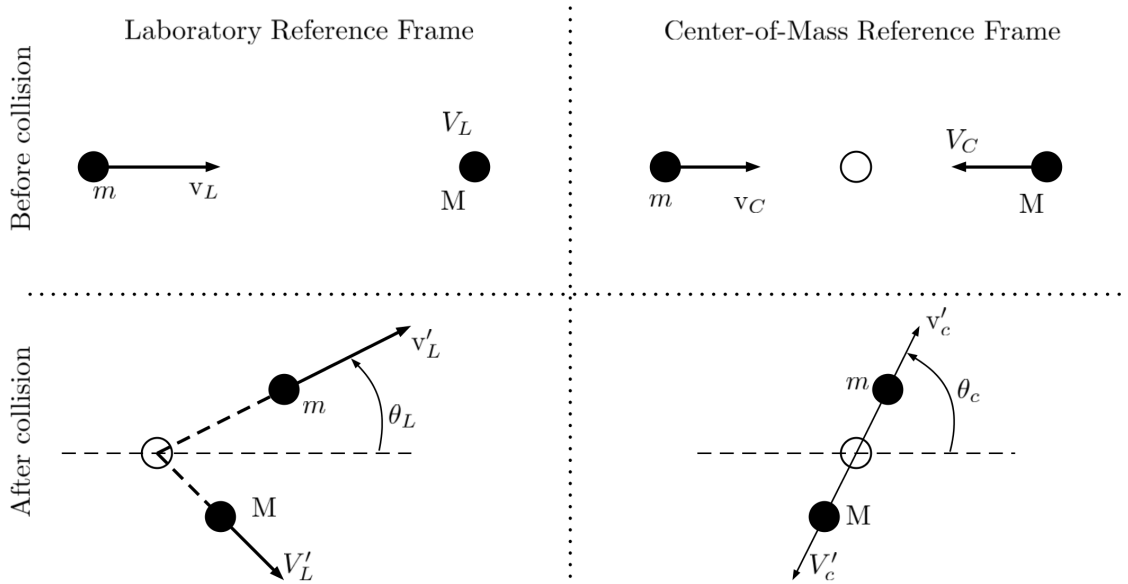## C.1 Simple particle-nuclide scattering processes

Figure C.1: Collision kinematics of a stationary nuclide in both the laboratory reference frame and the center-of-mass reference frame.

Let us consider a stationary target nucleus X_Z^A suspended in space and a particle moving towards this nucleus (from left to right) at velocity v_L, where L denotes the laboratory reference frame (i.e. the one we are living in) as denoted in Figure C.1. Assuming the target nucleas is at rest (an invalid assumption that will be treated later) with velocity V_L we know the energies associated with these particles to be

$$E_L = \frac{1}{2}m\mathrm{v}_L^2$$

$$E_{L_A} = \frac{1}{2}MV_L^2$$

where E_L is the energy of the particle and E_{L_A} is the energy of the target nucleus, both in the laboratory reference frame, and $m = 1$ is the mass of the particle and $M = A$ is the mass of the target nucleus. Fortunately the derivation of the mass-momentum equations relating the center-of-mass energies and angles to the laboratory reference frame quantities are comprehensively depicted in the textbook by Duderstadt and Hamilton [3]. In this book the scattering angle in the laboratory reference frame, θ_L, is related to the scattering angle in the center-of-mass reference frame, θ_c, as

$$\tan \theta_L = \frac{\sin \theta_c}{\frac{1}{A} + \cos \theta_c}. \tag{C.1}$$

Associated with this, [3] also derives the particle energy change $E_L \to E_L'$ as

$$E_L' = \left[\frac{(1+\alpha) + (1-\alpha)\cos \theta_c}{2} \right] E_L \tag{C.2}$$

where $\alpha = (\frac{A-1}{A+1})^2$. For light nuclei, where one can assume the scattering angle in the center-of-mass frame is isotropic [3] we can determine the probability distribution function for scattering through an angle θ_L. From equation C.1 we can get θ_L as

$$\theta_L = \begin{cases} \pi + \tan^{-1}\left(\frac{\sin \theta_c}{\frac{1}{A} + \cos \theta_c} \right) & \text{if } (\frac{1}{A} + \cos \theta_c) < 0 \\ \frac{\pi}{2} & \text{if } (\frac{1}{A} + \cos \theta_c) = 0 \\ \tan^{-1}\left(\frac{\sin \theta_c}{\frac{1}{A} + \cos \theta_c} \right) & \text{if } (\frac{1}{A} + \cos \theta_c) > 0 \end{cases} \tag{C.3}$$

Since $\cos \theta_c$, $\theta_c \in [0, \pi]$, is essentially our cumulative probability when linearly mapped to $[0, 1]$ we require the inverse of equation C.1. Therefore we begin by setting $x = \cos \theta_c$ and inserting it into equation C.3

$$\tan \theta_L = \frac{\sqrt{1-x^2}}{\frac{1}{A} + x}$$

and for simplicity we set the unknowns to constants

$$C = \frac{\sqrt{1-x^2}}{B+x}$$
$$C(B+x) = \sqrt{1-x^2}$$
$$C^2(x^2+2Bx+B^2) = 1-x^2$$
$$C^2x^2+2BC^2x+B^2C^2 = 1-x^2$$
$$(C^2+1)x^2+2BC^2x+B^2C^2-1 = 0$$

which is now in the familiar form $ax^2+bx+c = 0$ for which we complete the square to find

$$x = \frac{-2BC^2\pm\sqrt{4B^2C^4-4(C^2+1)(B^2C^2-1)}}{2(C^2+1)}$$
$$\therefore x = \frac{-2BC^2\pm 2C\sqrt{1-B^2+\frac{1}{C^2}}}{2(C^2+1)}.$$

The two possible x values obtained this way was incurred because we applied a square to remove the square-root term and therefore will give us the angle corresponding to $\tan\theta_L$ as well as $-\tan\theta_L$. Since we know that we started with a positive $\tan\theta_L$ we are only interested in the solution

$$\cos\theta_c = x = f(\theta_L) = g(\mu) = \frac{-2BC^2+2C\sqrt{1-B^2+\frac{1}{C^2}}}{2(C^2+1)}. \tag{C.4}$$

And therefore our mapping to a cumulative probability distribution becomes

$$\int_{-1}^{1} P(\mu).d\mu = \frac{g(\mu)-1}{2} \tag{C.5}$$

where $B=1/A$ and $C=\tan(\cos^{-1}\mu)$. The cumulative probability function for different masses of the target nucleus is shown in Figure C.2. Obtaining the probability density function, $P(\mu)$ is then a simple differentiation that can be done numerically

$$P(\mu) = \frac{1}{2}\frac{dg}{d\mu} \tag{C.6}$$

for which the results are shown in Figure C.3. The algorithm applied to find $P(\mu)$ is shown below

```
#----------------------------------------
def ThetaC(thetaL,A):
    B = 1/A
    if (thetaL == (math.pi/2)):
        C=1
    else:
        C = min(math.tan(thetaL),1.0e6)

    root = (1-B**2+1/(C**2))

    x1 = (-2*B*C**2 + 2*C*math.sqrt(root))/2/(C**2+1)
    #x2 = (-2*B*C**2 - 2*C*math.sqrt(root))/2/(C**2+1)
```

```
#Safety catches
if (x1>1.0):
    return math.acos(1)
if (x1<-1.0):
    return math.acos(-1)

return math.acos(x1)
```

```
#========================== Probability scattering mu
def Pmu(mu,A):
    thetaLA = math.acos(mu-0.0000001)
    thetaLB = math.acos(mu+0.0000001)
    thetacA = ThetaC(thetaLA,A)
    thetacB = ThetaC(thetaLB,A)
    CPLA    = 0.5-0.5*math.cos(thetacA)
    CPLB    = 0.5-0.5*math.cos(thetacB)
    return -(CPLB - CPLA)/0.0000002
```
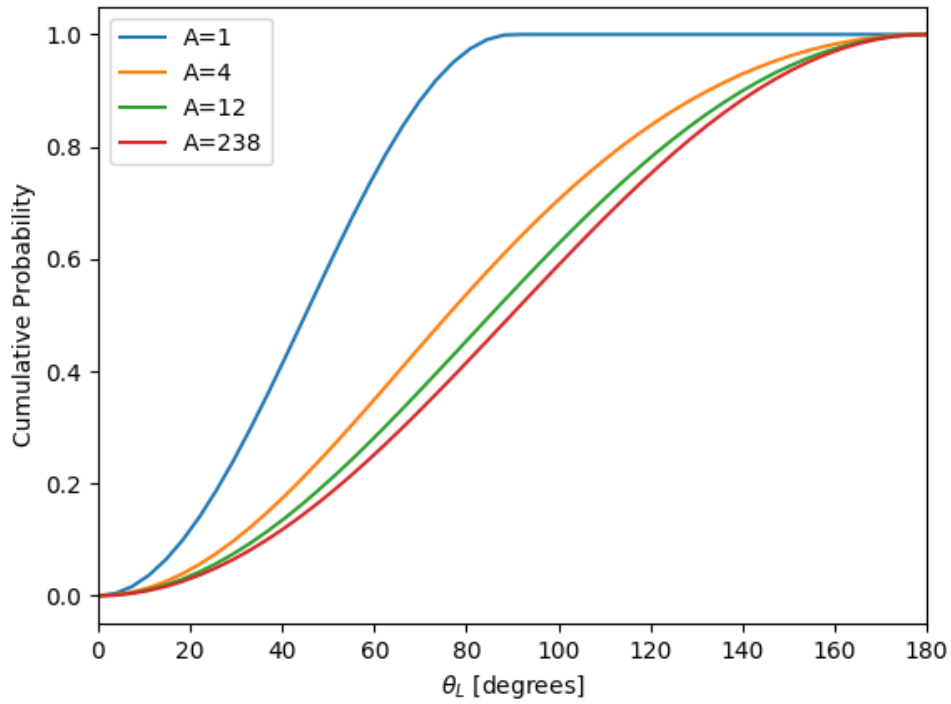

Figure C.2: Cumulative probability distribution for a particle scattering off a stationary nucleus of mass A.
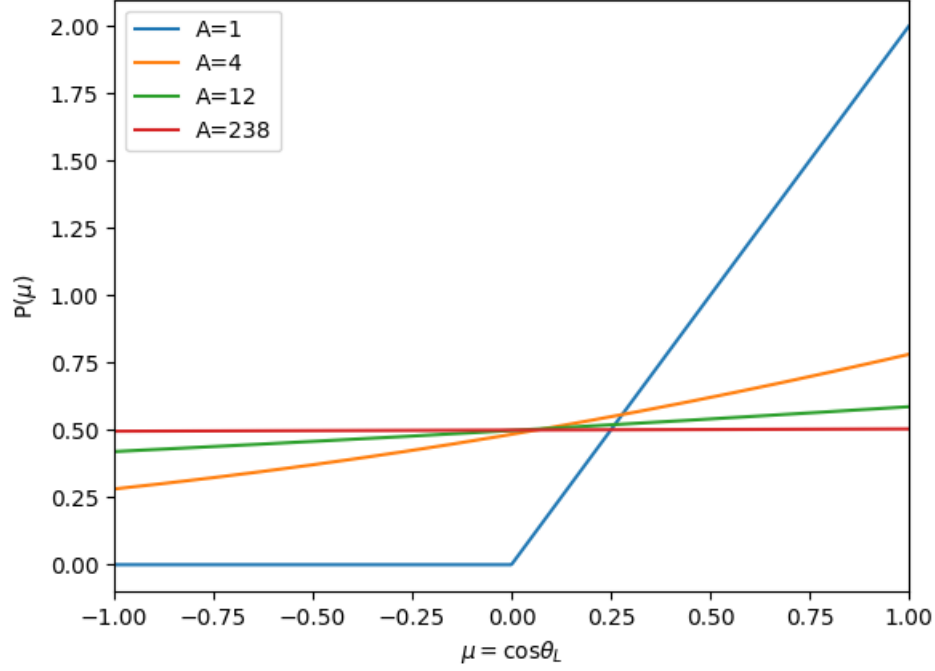
Figure C.3: Probability distribution for a particle scattering off a stationary nucleus of mass A.

C.2 Combining probabilities

Now, since μ corresponds to a discrete θ_c which also corresponds to a discrete $\frac{E'_L}{E_L}$, the kernel value $K(\mu, E' \rightarrow E)$ also will have only discrete points where it is non-zero, i.e.

$$K(\mu, E' \rightarrow E) = \begin{cases} P(\mu)P(E' \rightarrow E) & ,\text{if } E' - \left[\frac{(1+\alpha)+(1-\alpha)g(\mu)}{2}\right] E = 0 \\ 0 & ,otherwise \end{cases}$$

This discrete behavior requires significant numerical effort to resolve, however, multi-group integrations of the source- and destination energy groups alleviates this somewhat since

$$K(\mu, E_{g'} \rightarrow E_g) = \int_{E'_{g+1}}^{E'_g} \int_{E_{g+1}}^{E_g} K(\mu, E' \rightarrow E).dE.dE'$$

$$= P(\mu)P(E_{g'} \rightarrow E_g)$$

An algorithm to implement this kernel is shown below

```
def Kernel(mu,gprime,g,Eg,A,Ng=1000):
    #=== Bin boundaries
    Eiupp = Eg[gprime]
    Eilow = Eg[gprime+1]
    Efupp = Eg[g]
    Eflow = Eg[g+1]

    dEi = (Eiupp - Eilow)/Ng
    binWidth = (Efupp-Eflow)

    sumprobs=0
    thetaL = math.acos(mu)
    thetac = ThetaC(thetaL,A)
    muc = math.cos(thetac)
    for iE in range(0,Ng):
        Ein = Eilow + dEi/2 + dEi*iE
        Eout=Ef(muc,A,Ein)

        if ((Eout<=Efupp) and (Eout>=Eflow)):
            sumprobs = sumprobs + 1/Ng

    return sumprobs*Pmu(mu,A)
```

In order to test the multi-group implementation of this kernel we can build a simple 10 group energy discretization $E \in [0, 1]$ MeV with linearly spaced bins

```
G = 10
Eg = np.linspace(1,0,G+1)
```

The requirement here is that the continuous form obeys

$$\int_{-1}^{1} \int_{0}^{\infty} K(\mu, E' \to E).dE.d\mu = 1$$

and therefore the multi-group form must obey

$$\int_{-1}^{1} \left(\sum_{g=0}^{G} K(\mu, E_{g'} \to E_g) \right).d\mu = 1.$$

The code to implement this integration is

```
Np=100
mu=np.linspace(-0.9999,0.9999,Np)
ydis=np.zeros((Np))
sumofdis=0
sumovergroupsdis=0
for i in range(0,Np):
    for gdes in range(0,G):
        sumovergroupsdis=sumovergroupsdis+ \
                        Kernel(mu[i],gprime,gdes,Eg,A)*(2/Np)
```

and proves that the integral is unity as intended. Another test is to integrate over all angle with

$$\int_{4\pi} \left(\sum_{g=0}^{G} K(\Omega' \cdot \Omega, E_{g'} \to E_g) \right) .d\Omega'$$

$$= \int_{0}^{2\pi} \int_{0}^{\pi} \left(\sum_{g=0}^{G} K(\Omega' \cdot \Omega, E_{g'} \to E_g) \right) . \sin \theta' .d\theta' .d\varphi'$$

$$= 2\pi$$

where $\Omega' = [\sin\theta'.\cos\varphi', \sin\theta'.\sin\varphi', \cos\theta']$ and Ω is chosen arbitrarily (i.e. $\Omega = [1, 0, 0]$). The code to compute this integral, using the previous denoted 10-group energy structure, as well as scattering from group 0, is shown below

```python
Np = 100
Na = 200
polar = np.linspace(0.0001,math.pi*0.9999,Np)
azimu = np.linspace(0.0001,2*math.pi*0.99999,Na)
dtheta = (math.pi)/Np
dvarphi= (math.pi*2)/Na

nref = np.array([1.0,0.0,0.0])
ndir = np.array([0.0,0.0,0.0])

sumprob=0.0
gprime=0
for i in range(0,Na):
    print(i)
    for j in range(0,Np):
        varphi = azimu[i]
        theta  = polar[j]

        ndir[0] = math.sin(theta)*math.cos(varphi)
        ndir[1] = math.sin(theta)*math.sin(varphi)
        ndir[2] = math.cos(theta)

        mu = np.dot(ndir,nref)

        for gdes in range(0,G):
            sumprob=sumprob+ \
              Kernel(mu,gprime,gdes,Eg,A)*math.sin(theta)*dtheta*dvarphi
```

Indeed this does then integrate to 2π.

C.3   Legendre expansion of the scattering term

The discrete ordinates method involves the expansion of the scattering term using Legendre polynomials as basis functions. This expansion is of the form

$$K(\mu, E_{g'} \rightarrow E_g) = \sum_{\ell=0}^{\infty} \frac{2\ell+1}{2} P_\ell(\mu) K_\ell(E_{g'} \rightarrow E_g)$$

where the expansion coefficients are given by

$$K_\ell(E_{g'} \rightarrow E_g) = \int_{-1}^{1} K(\mu, E_{g'} \rightarrow E_g).P_\ell(\mu).d\mu$$

The code to compute the expansion coefficients requires just a small modification of the multi-group kernel in the sense that the Kernel is multiplied by the Legendre polynomial. The code is shown below

```python
def KernelL(ell,gprime,g,Eg,A):
    groupprob=0
    Np=800
    mu=np.linspace(-0.9999,0.9999,Np)
    dmu = (0.9999*2)/Np
    print("Integrating group %d to %d moment %d" %(gprime,g,ell))
    for i in range(0,Np):
        groupprob = groupprob + Kernel(mu[i],gprime,g,Eg,A)* \
            Legendre.Legendre(ell,mu[i])*dmu

    return groupprob
```

We can now decide to truncate our expansion at the L-th moment and precompute the expansion coefficient $K_\ell(E_{g'} \rightarrow E_g)$ with an example scattering from group $g' = 0$ to group $g = 1$ the code is

```python
L=10
KL=np.zeros((L+1))
gprime = 0
g=1
sumgroups=0
for ell in range(0,L+1):
    KL[ell] = KernelL(ell,gprime,g,Eg,A)
```

We can now compute the discrete and expanded form as a function of μ for which the code is shown below. A graphical plot of the expanded and discrete form is shown, for different orders of expansion, in Figure C.4.

```
#================================================= Discrete form vs Expansion for Group 0 to 1
Np=100
mu=np.linspace(-0.9999,0.9999,Np)
yexp=np.zeros((Np))
ydis=np.zeros((Np))
sumofdis=0
sumofexp=0
sumovergroupsdis=0
for i in range(0,Np):
    yexp[i] = expansion(L,mu[i],KL)
    ydis[i] = Kernel(mu[i],gprime,g,Eg,A)
    sumofexp=sumofexp+yexp[i]*(2/Np)
    sumofdis=sumofdis+ydis[i]*(2/Np)

    for gdes in range(0,G):
        sumovergroupsdis=sumovergroupsdis+ \
                        Kernel(mu[i],gprime,gdes,Eg,A)*(2/Np)
```
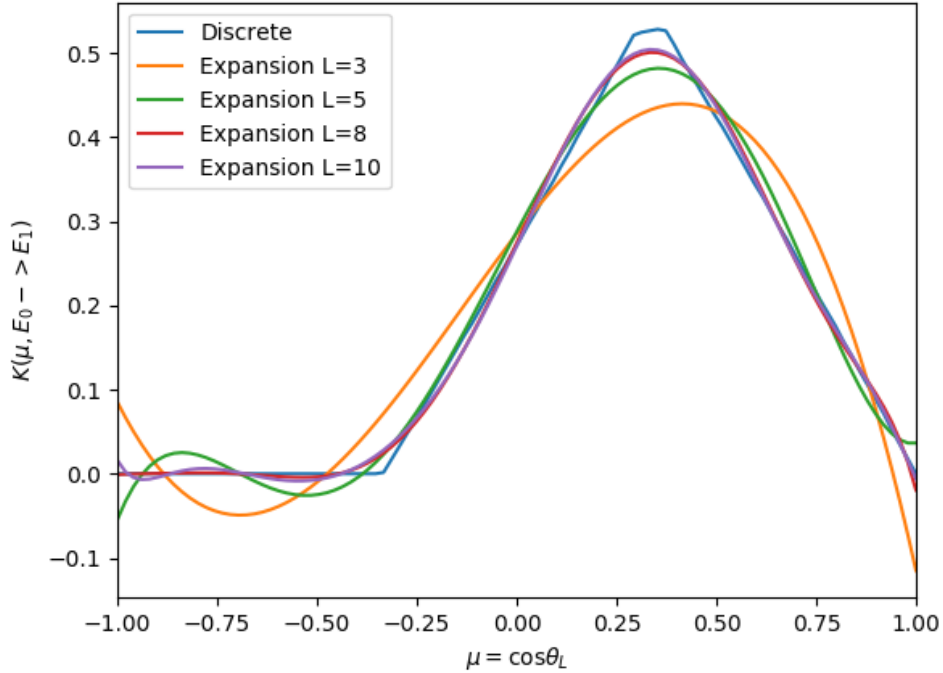

Figure C.4: Kernel function for a particle scattering off of a stationary carbon nuclear ($A = 12$) and scattering from group 0 to 1.

Appendix D   The Diffusion Approximation

D.1   Introductory elements

D.1.1   Current, J

The individual components of J, i.e., J_x, J_y, and J_z, are computed from an integration over all angles where the angular flux, $\psi(\mathbf{\Omega})$, is weighted with the respective angular cosine,

$$\mathbf{J} = \begin{bmatrix} J_x \\ J_y \\ J_z \end{bmatrix} = \begin{bmatrix} \int_{4\pi} \Omega_x \ \psi(\mathbf{\Omega}) \ d\mathbf{\Omega} \\ \int_{4\pi} \Omega_y \ \psi(\mathbf{\Omega}) \ d\mathbf{\Omega} \\ \int_{4\pi} \Omega_z \ \psi(\mathbf{\Omega}) \ d\mathbf{\Omega} \end{bmatrix} = \int_{4\pi} \mathbf{\Omega} \ \psi(\mathbf{\Omega}) \ d\mathbf{\Omega}. \tag{D.1}$$

This definition here is sufficient to introduce the concept of current, however, we will establish some relationships related to this definition.

D.1.2   Spherical harmonic expansion relation to $\mathbf{\Omega}$ and J

The first four spherical harmonics in the expansion

$$\psi(\mathbf{\Omega}) = \sum_{\ell=0}^{\infty} \frac{2\ell+1}{4\pi} \sum_{m=-\ell}^{+\ell} \phi_{\ell m} Y_{\ell e m}(\mathbf{\Omega})$$

are

$$Y_{0,0} = 1$$
$$Y_{1,-1} = \sin\theta \sin\varphi$$
$$Y_{1,0} = \cos\theta$$
$$Y_{1,1} = \sin\theta \cos\varphi.$$

The last three harmonics have a relationship with $\mathbf{\Omega}$ as

$$\mathbf{\Omega} = \begin{bmatrix} \Omega_x \\ \Omega_y \\ \Omega_z \end{bmatrix} = \begin{bmatrix} \sin\theta\cos\varphi \\ \sin\theta\sin\varphi \\ \cos\theta \end{bmatrix} = \begin{bmatrix} Y_{1,1} \\ Y_{1,-1} \\ Y_{1,0} \end{bmatrix} \tag{D.2}$$

And the accompanying first four expansion coefficients, rearranged according to the relationship with $\mathbf{\Omega}$,

are determined from

$$\phi_{0,0} = \int_{4\pi} \psi(\mathbf{\Omega}) Y_{0,0} \, d\mathbf{\Omega}$$

$$\phi_{1,-1} = \int_{4\pi} \psi(\mathbf{\Omega}) Y_{1,-1} \, d\mathbf{\Omega}$$

$$\phi_{1,1} = \int_{4\pi} \psi(\mathbf{\Omega}) Y_{1,1} \, d\mathbf{\Omega}$$

$$\phi_{1,0} = \int_{4\pi} \psi(\mathbf{\Omega}) Y_{1,0} \, d\mathbf{\Omega}$$

after which we substitute the components of $\mathbf{\Omega}$ to get

$$\phi_{0,0} = \int_{4\pi} \psi(\mathbf{\Omega}) Y_{0,0} \, d\mathbf{\Omega}$$

$$\begin{bmatrix} \phi_{1,1} \\ \phi_{1,-1} \\ \phi_{1,0} \end{bmatrix} = \begin{bmatrix} \int_{4\pi} \Omega_x \, \psi(\mathbf{\Omega}) \, d\mathbf{\Omega} \\ \int_{4\pi} \Omega_y \, \psi(\mathbf{\Omega}) \, d\mathbf{\Omega} \\ \int_{4\pi} \Omega_z \, \psi(\mathbf{\Omega}) \, d\mathbf{\Omega} \end{bmatrix} = \int_{4\pi} \mathbf{\Omega} \, \psi(\mathbf{\Omega}) \, d\mathbf{\Omega} = \mathbf{J}$$

D.1.3 Linear in angle assumption

With some rearrangement, the expansion truncated at $\ell = 1$ yields

$$\psi(\mathbf{\Omega}) \approx \frac{1}{4\pi} \phi_{0,0} + \frac{3}{4\pi} \begin{bmatrix} Y_{1,1} \\ Y_{1,-1} \\ Y_{1,0} \end{bmatrix} \cdot \begin{bmatrix} \phi_{1,1} \\ \phi_{1,-1} \\ \phi_{1,0} \end{bmatrix}$$

after which we can substitute the expressions for $\mathbf{\Omega}$ as well as the current

$$\psi(\mathbf{\Omega}) \approx \frac{1}{4\pi} \phi_{0,0} + \frac{3}{4\pi} \mathbf{\Omega} \cdot \mathbf{J} \tag{D.3}$$

D.1.4 Other mathematical identities

No effort was given here to deriving the angular integration identities since they can become quite messy. For those interested: one piece of advice is write out the vectors, with $\mathbf{\Omega}$ in φ-and-μ form, and perform the integrals on a component-by-component basis. It is also easy to make a mistake, so use wolfram-alpha or a similar resource to assist.

Identity D-1

$$\int_{4\pi} d\mathbf{\Omega} = 4\pi.$$

Identity D-2

$$\int_{4\pi} \mathbf{\Omega} \, d\mathbf{\Omega} = 0.$$

Identity D-3 Given the known three component vector, $\mathbf{v}$,

$$\int_{4\pi} \mathbf{\Omega}\cdot\mathbf{v} \; d\mathbf{\Omega} = 0.$$

Identity D-4 Given the known three component vector, $\mathbf{v}$,

$$\int_{4\pi} \mathbf{\Omega}\cdot\mathbf{\nabla}(\mathbf{\Omega}\cdot\mathbf{v}) \; d\mathbf{\Omega} = \frac{4\pi}{3}\mathbf{\nabla}\cdot\mathbf{v}.$$

Identity D-5 Given the scalar, a,

$$\int_{4\pi} \mathbf{\Omega}\left(\mathbf{\Omega}\cdot\mathbf{\nabla}a\right) \; d\mathbf{\Omega} = \frac{4\pi}{3}\mathbf{\nabla}a.$$

Identity D-6 Given the known three component vector, $\mathbf{v}$,

$$\int_{4\pi} \mathbf{\Omega}\left(\mathbf{\Omega}\cdot\mathbf{v}\right) \; d\mathbf{\Omega} = \frac{4\pi}{3}\mathbf{v}.$$

Identity D-7 Given the known three component vector, $\mathbf{v}$,

$$\int_{4\pi} \mathbf{\Omega}\left(\mathbf{\Omega}\cdot\mathbf{\nabla}(\mathbf{\Omega}\cdot\mathbf{v})\right) \; d\mathbf{\Omega} = 0.$$

D.2 Linear approximation in the transport equation

When we substitute the linear in angle approximation for the angular flux into the transport equation,

$$\left(\mathbf{\Omega}\cdot\nabla+\sigma_{tg}(\mathbf{x})\right)\psi_g(\mathbf{x},\mathbf{\Omega}) = \sum_{m=0}^{m_{max}}\frac{2\ell+1}{4\pi}Y_{\ell m^*}(\mathbf{\Omega})\sum_{g'=0}^{G-1}\left[\sigma_{sm,g'\to g}(\mathbf{x}).\phi_{mg'}(\mathbf{x})\right]+\frac{q_g(\mathbf{x})}{4\pi}, \qquad (D.4)$$

we get

$$\left(\mathbf{\Omega}\cdot\nabla+\sigma_{tg}(\mathbf{x})\right)\left[\frac{1}{4\pi}\phi_{0g}(\mathbf{x})+\frac{3}{4\pi}\mathbf{\Omega}\cdot\mathbf{J}_g(\mathbf{x})\right] = \sum_{g'=0}^{G-1}\left[\frac{1}{4\pi}\sigma_{s0,g'\to g}(\mathbf{x})\phi_{0g'}(\mathbf{x})+\frac{3}{4\pi}\sigma_{s1,g'\to g}\mathbf{\Omega}\cdot\mathbf{J}_g(\mathbf{x})\right]+\frac{q_g(\mathbf{x})}{4\pi}. \tag{D.5}$$

We now integrate this equation over all angle space (i.e., $\int_{4\pi} d\mathbf{\Omega}$). We first expand the left-hand side of eq. D.5:

$$\left(\mathbf{\Omega}\cdot\nabla+\sigma_{tg}(\mathbf{x})\right)\left[\frac{1}{4\pi}\phi_{0g}(\mathbf{x})+\frac{3}{4\pi}\mathbf{\Omega}\cdot\mathbf{J}_g\right]$$
$$= \frac{1}{4\pi}\mathbf{\Omega}\cdot\mathbf{\nabla}\phi_{0g}(\mathbf{x})+\frac{1}{4\pi}\sigma_{tg}\phi_{0g}(\mathbf{x})+\frac{3}{4\pi}\mathbf{\Omega}\cdot\mathbf{\nabla}\left(\mathbf{\Omega}\cdot\mathbf{J}_g(\mathbf{x})\right)+\frac{3}{4\pi}\sigma_{tg}\mathbf{\Omega}\cdot\mathbf{J}_g(\mathbf{x}),$$

and now apply the angular integration so that

$$\int_{4\pi}\left[\frac{1}{4\pi}\mathbf{\Omega}\cdot\mathbf{\nabla}\phi_{0g}(\mathbf{x})+\frac{1}{4\pi}\sigma_{tg}\phi_{0g}(\mathbf{x})+\frac{3}{4\pi}\mathbf{\Omega}\cdot\mathbf{\nabla}\left(\mathbf{\Omega}\cdot\mathbf{J}_g(\mathbf{x})\right)+\frac{3}{4\pi}\sigma_{tg}\mathbf{\Omega}\cdot\mathbf{J}_g(\mathbf{x})\right]d\mathbf{\Omega}$$
$$= \sigma_{tg}\phi_{0g}(\mathbf{x})+\mathbf{\nabla}\cdot\mathbf{J}_g(\mathbf{x}),$$

where the first and second terms integrate to zero according to identity D-3, and the third term reduces to a divergence term via identity D-4. We now do the same to the right hand side of eq. D.5:

$$
\int_{4\pi}\left[\sum_{g'=0}^{G-1}\left[\frac{1}{4\pi}\sigma_{s0,g'\to g}(\mathbf{x})\phi_{0g'}(\mathbf{x})+\frac{3}{4\pi}\sigma_{s1,g'\to g}\mathbf{\Omega\cdot J}_g(\mathbf{x})\right]+\frac{q_g(\mathbf{x})}{4\pi}\right]d\mathbf{\Omega}
$$

$$
=\sum_{g'=0}^{G-1}\sigma_{s0,g'\to g}(\mathbf{x})\phi_{0g'}(\mathbf{x})+q_g(\mathbf{x}),
$$

after which we reconcile the left- and right-hand sides to produce

$$
\mathbf{\nabla\cdot J}_g(\mathbf{x})+\sigma_{tg}\phi_{0g}(\mathbf{x})=\sum_{g'=0}^{G-1}\sigma_{s0,g'\to g}(\mathbf{x})\phi_{0g'}(\mathbf{x})+q_g(\mathbf{x}),\tag{D.6}
$$

which still leaves a unresolved $\mathbf{J}$ term. This term requires the definition of another equation which we obtain by multiplying eq. D.5 by $\mathbf{\Omega}$ and again integrate over angle space. To show how this is done we again start with the expansion of the left-hand side but, this time around, we multiply with $\mathbf{\Omega}$,

$$
\mathbf{\Omega}\left(\mathbf{\Omega\cdot\nabla}+\sigma_{tg}(\mathbf{x})\right)\left[\frac{1}{4\pi}\phi_{0g}(\mathbf{x})+\frac{3}{4\pi}\mathbf{\Omega\cdot J}_g\right]
$$

$$
=\frac{1}{4\pi}\mathbf{\Omega}\left(\mathbf{\Omega\cdot\nabla}\phi_{0g}(\mathbf{x})\right)+\frac{1}{4\pi}\mathbf{\Omega}\sigma_{tg}\phi_{0g}(\mathbf{x})+\frac{3}{4\pi}\mathbf{\Omega}\left[\mathbf{\Omega\cdot\nabla}\left(\mathbf{\Omega\cdot J}_g(\mathbf{x})\right)\right]+\frac{3}{4\pi}\mathbf{\Omega}\left(\sigma_{tg}\mathbf{\Omega\cdot J}_g(\mathbf{x})\right),
$$

we then again apply the integration over angle space to get

$$
\int_{4\pi}\left[\frac{1}{4\pi}\mathbf{\Omega}\left(\mathbf{\Omega\cdot\nabla}\phi_{0g}(\mathbf{x})\right)+\frac{1}{4\pi}\mathbf{\Omega}\sigma_{tg}\phi_{0g}(\mathbf{x})+\frac{3}{4\pi}\mathbf{\Omega}\left[\mathbf{\Omega\cdot\nabla}\left(\mathbf{\Omega\cdot J}_g(\mathbf{x})\right)\right]+\frac{3}{4\pi}\mathbf{\Omega}\left(\sigma_{tg}\mathbf{\Omega\cdot J}_g(\mathbf{x})\right)\right]d\mathbf{\Omega}
$$

$$
=\frac{1}{3}\mathbf{\nabla}\phi_{0g}(\mathbf{x})+\sigma_{tg}\mathbf{J}_g(\mathbf{x})
$$

where the first term has reduced to a gradient term according to identity D-5, the second term integrates to zero via identity 1, the third term integrates to zero via identity D-7 and the last term has reduced to just a current term via identity D-6. Doing the same to the right-hand side,

$$
\int_{4\pi}\mathbf{\Omega}\left[\sum_{g'=0}^{G-1}\left[\frac{1}{4\pi}\sigma_{s0,g'\to g}(\mathbf{x})\phi_{0g'}(\mathbf{x})+\frac{3}{4\pi}\sigma_{s1,g'\to g}\mathbf{\Omega\cdot J}_g(\mathbf{x})\right]+\frac{q_g(\mathbf{x})}{4\pi}\right]d\mathbf{\Omega}
$$

$$
=\sum_{g'=0}^{G-1}\sigma_{s1,g'\to g}(\mathbf{x})\mathbf{J}_{g'}(\mathbf{x}),
$$

where the first and last term has been eliminated via identity D-1. After reconstituting the left- and right-hand sides we get

$$
\frac{1}{3}\mathbf{\nabla}\phi_{0g}(\mathbf{x})+\sigma_{tg}\mathbf{J}_g(\mathbf{x})=\sum_{g'=0}^{G-1}\sigma_{s1,g'\to g}(\mathbf{x})\mathbf{J}_{g'}(\mathbf{x}).\tag{D.7}
$$

We now make an approximation which ought not to be intuitive. We assume that the sum over group g' of the product of the first moment of the scattering cross-section, from g' to g, and the current $\mathbf{J}_{g'}$ can be approximated as

$$\sum_{g'=0}^{G-1} \sigma_{s1,g'\to g}\mathbf{J}_{g'} \approx \sum_{g'=0}^{G-1} \sigma_{s1,g\to g'}\mathbf{J}_{g}. \tag{D.8}$$

When substituted into our second equation for $\mathbf{J}$ we get

$$\frac{1}{3}\boldsymbol{\nabla}\phi_{0g}(\mathbf{x})+\sigma_{tg}\mathbf{J}_g(\mathbf{x}) = \sum_{g'=0}^{G-1} \sigma_{s1,g\to g'}\mathbf{J}_{g}$$

$$\mathbf{J}_g\left(\sigma_{tg}-\sum_{g'=0}^{G-1} \sigma_{s1,g\to g'}\right) = -\frac{1}{3}\boldsymbol{\nabla}\phi_{0g}(\mathbf{x}). \tag{D.9}$$

For simplicity we then define the transport corrected diffusion coefficient,

$$D_g(\mathbf{x}) = \frac{1}{3\left(\sigma_{tg}-\displaystyle\sum_{g'=0}^{G-1} \sigma_{s1,g\to g'}\right)},$$

after which the equation above becomes

$$\mathbf{J}_g = -D_g\boldsymbol{\nabla}\phi_{0g}(\mathbf{x}).$$

When we substitute this for $\mathbf{J}_g$ in eq. D.2 we get the familiar diffusion-equation form,

$$-\boldsymbol{\nabla}\cdot D_g\boldsymbol{\nabla}\phi_{0g}(\mathbf{x})+\sigma_{tg}\phi_{0g}(\mathbf{x}) = \sum_{g'=0}^{G-1} \sigma_{s0,g'\to g}(\mathbf{x})\phi_{0g'}(\mathbf{x})+q_g(\mathbf{x}). \tag{D.10}$$

References

[1] Lewis E.E, Miller W.F. *Computational Methods of Neutron Transport*, John Wiley & Sons, 1984, ISBN 0-471-09245-2

[2] Barrera-Figueroa V., et al. *Multiple root finder algorithm for Legendre and Chebyshev polynomials via Newton's method*, Annales Mathematicae et Informaticae, volume 33, pages 3-13, 2006

[3] Duderstadt J.J., Hamilton L.J., *Nuclear Reactor Analysis*, John Wiley & Sons, 1976.